Quaternary International 695 (2024) 31–44

Contents lists available at ScienceDirect

Quaternary International

journal homepage: www.elsevier.com/locate/quaint

Postglacial vegetation and climate change in the Lake Onega region of eastern Fennoscandia derived from a radiocarbon-dated pollen record

Aleksandra I. Krikunova [a,*], Larisa A. Savelieva [b], Tengwen Long [c,d], Christian Leipe [a,e,f], Franziska Kobe [a], Natalia A. Kostromina [a,b,g], Aleksandra V. Vasilyeva [b], Pavel E. Tarasov [a,**]

[a] Institute of Geological Sciences, Palaeontology Section, Freie Universität Berlin, Malteserstraße 74–100, Building D, 12249, Berlin, Germany
[b] Institute of Earth Sciences, St. Petersburg State University, Universitetskaya Naberezhnaya 7/9, St. Petersburg 199034, Russia
[c] School of Geographical Sciences, University of Nottingham Ningbo China, 199 Taikang East Road, Yinzhou District, Ningbo, Zhejiang, 315100, China
[d] Key Laboratory of Carbonaceous Wastes Processing and Process Intensification Research of Zhejiang Province, University of Nottingham Ningbo China, 199 Taikang East Road, Yinzhou District, Ningbo, Zhejiang, 315100, China
[e] Domestication and Anthropogenic Evolution Research Group, Max Planck Institute of Geoanthropology, Kahlaische Str. 10, 07745, Jena, Germany
[f] Department of Archaeology, Max Planck Institute of Geoanthropology, Kahlaische Str. 10, 07745, Jena, Germany
[g] VNIIOkeanologia, Angliyskiy Prospekt 1, St. Petersburg 190121, Russia

ARTICLE INFO

Keywords:
Pollen record
Biome reconstruction
8.2 ka BP event
Northgrippian-Meghalayan transition
Karelia

ABSTRACT

With its numerous environmental archives stored in lake and peat sediments and relatively low human pressure, the Lake Onega region in eastern Fennoscandia is regarded as a particularly promising area for studying past changes in vegetation and climate since the Lateglacial period. The 885-cm-long sediment core RZ19 (62°27′53″N, 34°26′4″E) was collected from Razlomnoe Peat on the northern shore of Lake Onega in 2019, radiocarbon-dated and analysed for pollen and cryptogam spores. The age-depth model suggests continuous sedimentation since ca. 11,800 a BP (all ages given in years (a) or kiloyears (ka) before present (BP) with BP referring to 1950 CE). The results of pollen analysis and pollen-based biome reconstruction show rapid afforestation of the area in the Early Holocene, although the scores of the tundra biome remain relatively high prior to ca. 11,450 a BP, suggesting that the vegetation was likely more open than today. Between 8300 and 8000 a BP, *Betula* sect. *Albae* shows a marked increase in pollen percentage, while *Pinus sylvestris* experiences a marked decrease. These changes coinciding with the 8.2 ka BP cooling event indicate less favourable conditions for Scots pine while being beneficial for fast-growing birch. The transition from the Early to Middle Holocene (i.e. from Greenlandian to Northgrippian) is marked by an increase in pollen productivity, spread of *Picea* and further afforestation of the area. The decrease in arboreal and *Picea* pollen percentages and the abrupt increase in landscape openness after ca. 4000 a BP mark the onset of the Late Holocene (i.e. Northgrippian-Meghalayan transition) and likely reflect the combined effect of insolation-induced temperature decrease and associated paludification and forest retreat rather than a decrease in atmospheric precipitation and/or spread of Late Neolithic agriculture.

1. Introduction

Eastern Fennoscandia, encompassing Karelia and the Kola Peninsula in Russia, Finland and northeastern Norway (Fig. 1a), has a long tradition of palaeoenvironmental studies focused on deglaciation history (e.g. Lunkka et al., 2018; Stroeven et al., 2016); postglacial vegetation dynamics (e.g. Berglund et al., 1996; Elina et al., 2010; Velichko et al., 2017; Väliranta et al., 2011); and proxy-based climate reconstructions (e.g. Eräsẗo et al., 2012; Meyer-Jacob et al., 2017; Nazarova et al., 2020; Plikk et al., 2019; Seppä et al., 2007, 2009). The results obtained from single-site studies were successfully used in a large number of regional to global-scale palaeoecological projects and for comparisons with the results of Earth system modelling experiments (e.g. Giesecke and Bennett, 2004; Hughes et al., 2016; Kaufman and Broadman, 2023; Prentice et al., 1996; Roberts et al., 2018).

Another topic showing steadily growing scientific interest in recent

* Corresponding author.
** Corresponding author.
E-mail addresses: aleksandra.krikunova@fu-berlin.de (A.I. Krikunova), ptarasov@zedat.fu-berlin.de (P.E. Tarasov).

https://doi.org/10.1016/j.quaint.2024.04.003
Received 24 January 2024; Received in revised form 29 March 2024; Accepted 4 April 2024
Available online 19 April 2024

years is the prehistoric population history of eastern Fennoscandia, human-environment interactions and human responses to past climatic change (e.g. Alenius et al., 2021; Gerasimov and Kriiska, 2018; Kotlyakov et al., 2017; Manninen et al., 2018; Tallavaara et al., 2010). Progress in this area of research is largely based on high-resolution environmental archives and an interdisciplinary approach to archaeology, but not least on the widespread use of Accelerator Mass Spectrometry (AMS) radiocarbon (^{14}C) dating and Bayesian modelling, considering corrections for freshwater reservoir effects (e.g. Bronk Ramsey et al., 2014).

Studies aimed at reconstructing the Lateglacial-Holocene environment (e.g. Harrison et al., 1996; Tarasov et al., 1998; Wohlfarth et al., 2007) and the impacts of past climate changes on human populations (e.g. Schulting et al., 2022) demonstrated the importance of pollen data from the Lake Onega region (LOR). However, problems associated with most of the published records (Supplementary Table S1) include coarse resolution and lack of robust age control, which challenge identification of hiatuses and regional/interregional correlations. With a few exceptions, which demonstrate the results of international collaboration projects of the past two decades (e.g. Nazarova et al., 2020; Schulting et al., 2022; Tarasov et al., 2017; Wohlfarth et al., 2002, 2004), archaeological and palaeoenvironmental chronologies refer to uncalibrated ^{14}C ages and pollen-based correlations with the Blytt–Sernander bioclimatic classification adapted to Northern Eurasia (e.g. Filimonova and Lavrova, 2017). In contrast, the sensitivity of regional vegetation to the 8.2 and 4.2 ka climatic events dating back to ca. 8200 and 4200 a BP and representing the Early to Middle and Middle to Late Holocene transitions were not the focus of earlier studies.

In the current paper, we present the new ^{14}C-dated RZ19 pollen record from Razlomnoe Peat recovered in 2019, which shows continuous sedimentation during the past ca. 11.8 ka BP. The obtained results of pollen analysis and quantitative biome reconstruction are discussed in terms of reconstructed changes in regional vegetation cover and composition; its sensitivity to postglacial climate dynamics in the North Atlantic region, with a focus on the 8.2 and 4.2 ka BP climatic events; and the main geostratigraphic transitions of the Holocene epoch.

2. Regional setting and modern environments

Lake Onega (Fig. 1b) is situated in the southeasternmost part of Fennoscandia (Fig. 1a), at the geological contact between the Baltic Shield composed of Archean and Proterozoic gneisses and greenstone and the East European Platform (Alpat'ev et al., 1976). It was covered by the Scandinavian Ice Sheet (SIS) during the last glacial period ca. 20 ka BP (Stroeven et al., 2016; Svendsen et al., 2004). The deglaciation of the area began after ca. 15 ka BP and the SIS limit (both maximum and most credible scenario) was north of the lake about 12 ka BP (Hughes et al., 2016, Fig. 1c and d). Saarnisto and Saarinen (2001) concluded that Lake Onega was deglaciated ca. 14 ka BP based on varve counts, although the exact timing is still debated (e.g. Demidov, 2005, 2006; Filatov, 2010).

The area around the lake experiences humid, summer-warm, moderately continental climate (Kottek et al., 2006, Table 1) with a predominance of air masses of Atlantic and Arctic origin throughout the year (Alpat'ev et al., 1976). The mean temperatures vary from −13 to −8.4 °C in January and from 16 to 17.6 °C in July (Table 1). Annual precipitation in the catchment ranges between 550 and 750 mm, reaching a maximum in the summer months (Sharov et al., 2014). Reflecting the modern climate warming, instrumental records (Table 1) from representative weather stations (Fig. 1b) demonstrate a distinct increase in July and January temperature for the period 1991–2020 compared to the 1961–1990 interval. The increase in temperature is accompanied by an increase in precipitation at lake shore stations

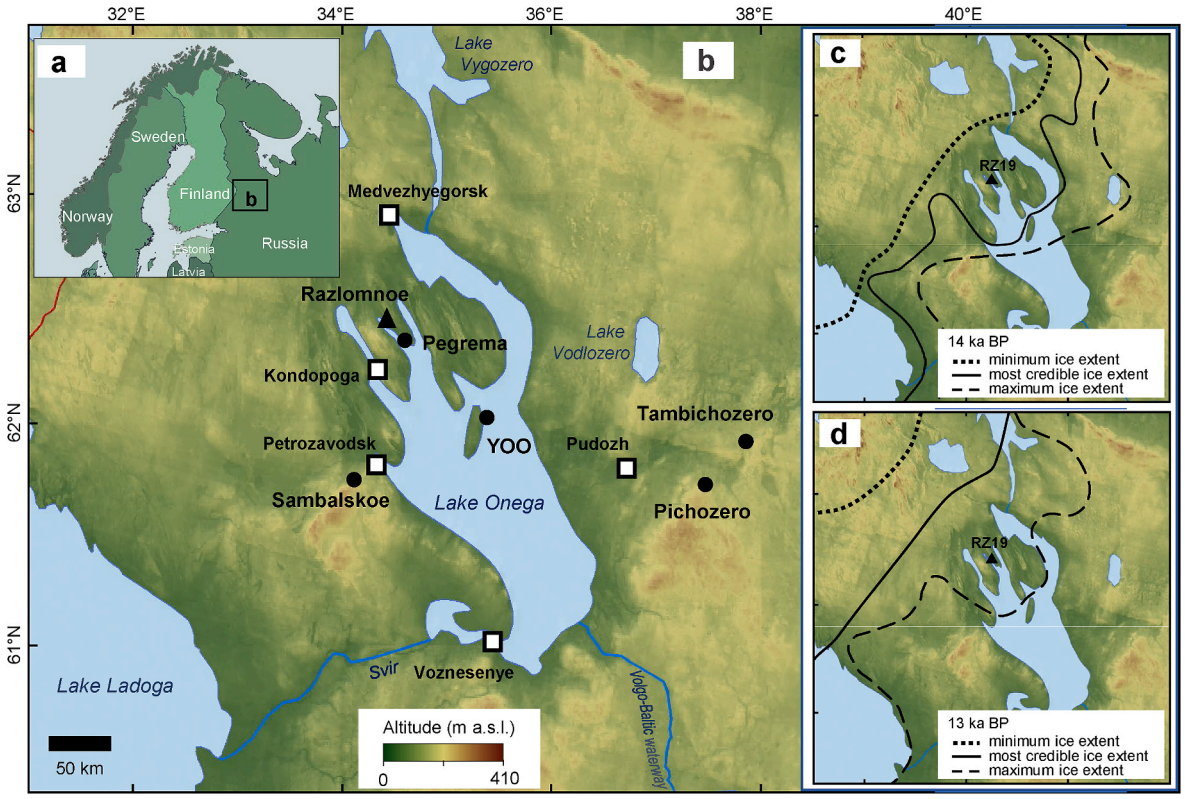

Fig. 1. (a) Overview map showing the location of eastern Fennoscandia and the Lake Onega region (black rectangle) in northern Europe; (b) topographic map of the study region with hydrology and location of Razlomnoe Peat and the RZ19 sediment core (black triangle) along with other key sites from the region used in the discussion (black dots) and representative meteorological stations (white squares); and DATED-1 time-slice reconstructions of the extent of the Scandinavian ice sheet in the study region at (c) 14 and (d) 13 ka BP (after Hughes et al., 2016). Three lines indicate maximum, minimum and most credible ice extent to represent uncertainty in the data.

Table 1
Mean January and July temperatures and annual precipitation sums at five representative stations around Lake Onega (Fig. 1b), averaged over the period 1961–1990 and 1991–2020 (this study).

Station name and location	Interval (years)	Mean January temp. (°C)	Mean July temp. (°C)	Ann. precip. (mm)	Reference (accessed June 04, 2023)
Medvezhyegorsk	1961–1990	−12.9	16.0	670	http://www.pogodaiklimat.ru/history/22721.htm
62.92°N, 34.43°E, 81 m a.s.l.	*1991–2020*	*−9.7*	*16.9*	*766*	http://www.pogodaiklimat.ru/history/22721_2.htm
Kondopoga	1961–1990	−11.9	16.6	547	http://www.pogodaiklimat.ru/history/22727.htm
62.17°N, 34.30°E, 38 m a.s.l.	*1991–2020*	*−8.7*	*17.5*	*632*	http://www.pogodaiklimat.ru/history/22727_2.htm
Petrozavodsk	1961–1990	−11.4	16.0	592	http://www.pogodaiklimat.ru/history/22820.htm
61.82°N, 34.27°E, 111 m a.s.l.	*1991–2020*	*−8.4*	*17.1*	*612*	http://www.pogodaiklimat.ru/history/22820_2.htm
Voznesenye	1961–1990	−11.6	16.3	limited data	http://www.pogodaiklimat.ru/history/22829.htm
61.02°N, 35.48°E, 41 m a.s.l.	*1991–2020*	*−8.4*	*17.4*	*715*	http://www.pogodaiklimat.ru/history/22829_2.htm
Pudozh	1961–1990	−13.2	16.4	732	http://www.pogodaiklimat.ru/history/22831.htm
61.80°N, 36.52°E, 44 m a.s.l.	*1991–2020*	*−10.0*	*17.6*	*731*	http://www.pogodaiklimat.ru/history/22831_2.htm

(Table 1), possibly due to increased evaporation from the lake surface.

The lake is situated in a climate-sensitive area at the bioclimatic border between the boreal conifer forest (taiga) biome and the cool conifer forest biome (Prentice et al., 1996). The predominant tree taxa are Scots pine (*Pinus sylvestris*), spruce (*Picea abies*, *P. obovata*) and birch (*Betula pendula*, *B. pubescens*) trees followed by aspen (*Populus tremula*) and alder (*Alnus incana*, *A. glutinosa*) species (Alpat'ev et al., 1976; Lindholm et al., 2015). The cool conifer forest biome (called 'southern taiga' in the Russian botanical literature) spreads south of 60°N (Fig. 2). It is characterised by the frequent appearance of temperate deciduous taxa such as linden (*Tilia cordata*), elm (*Ulmus glabra*, *U. laevis*), oak (*Quercus robur*) and hazel (*Corylus avellana*), although individual elm and linden trees grow near Lake Onega and on its islands in places with the most fertile soils and a milder microclimate (e.g. Filimonova and Lavrova, 2015; Sokolov et al., 1986, Fig. 2). The forest understory is typically composed of birch and willow shrubs and semi-shrubs (members of Ericales and Rosaceae are the most common), grasses (Poaceae), sedges (Cyperaceae), various herbs, mosses and lichens (Alpat'ev et al., 1976). Wet habitats, including marshes, fens and ombrotrophic bogs with *Sphagnum* mosses, sedges and dwarf shrubs (e.g. *B. nana*) are well represented in the landscape (Lindholm et al., 2015) and resemble tundra environments. The human impact on the landscape is minor outside the towns and settlements. Petrozavodsk is the largest city in the region with a population of about 280,000, while most of the territory is sparsely populated.

3. Material and methods

3.1. Study site, sediment coring and subsampling

Razlomnoe (53 m a.s.l.) is a NW–SE-oriented nutrient-rich riparian peat (Fig. 1b) with a surface area of ca. 0.2 km^2, approximately 2 km long and 0.1 km wide in the central part. The peat occupies a depression that was once a bay of Lake Onega (Elina and Khomutova, 1987) and has a complex bedrock morphology (Shevelin et al., 1988). The surrounding area is low-elevated (Fig. 1b) with relative altitude variations up to 100 m caused by the alternation of narrow submeridional ridges (*selkä*) and interridge depressions occupied by peats and freshwater lakes formed after the deglaciation of the territory (Lindholm et al., 2015).

Coring of the peat (Fig. 1b) for the purposes of this study was carried out using a hand-held peat corer (5 cm in diameter) with a 100-cm-long sampler. The 885-cm-long sediment core RZ19 was recovered from the site (62°27′53″N, 34°26′4″E) with the maximal thickness of the undisturbed peat layer in the central part of the peat bog. The core material was transported to the pollen laboratory of St. Petersburg State University, where it was stored at a low temperature for further analysis. The core lithology was first described in the field and refined in the laboratory.

3.2. ^{14}C dating and core chronology

A total of 10 bulk sediment samples (Table 2) were ^{14}C-dated in the Radiocarbon Laboratory at St. Petersburg University (conventional approach) and in the Poznan Radiocarbon Laboratory (AMS dating). We calibrated all ^{14}C ages using the IntCal20 calibration curve (Reimer et al., 2020) in OxCal v.4.4 (Bronk Ramsey, 1995). The age-depth relationship of the sequence was modelled in rbacon software package v.3.2.0 (Blaauw and Christen, 2011) on the R v.4.3.2 platform (R Core Team, 2016). The package rbacon uses Bayesian approaches for chronological modelling allowing incorporation of prior knowledge on the changes of stratigraphy or sedimentation rate into the model (Wang et al., 2019). Three dates that lead to obvious age-depth reversals were not used in the model: LU-10200, LU-10201, and Poz-140075.

Two stratigraphical tie points (STPs) were introduced to the modelling (Fig. 3) based on the lithostratigraphy of the sediment profile and the regional pollen stratigraphy (e.g. Krikunova et al., 2022; Lenz et al., 2021; Wohlfarth et al., 2004). The top of the sequence (i.e. 0 cm depth) was constrained to −69 a BP (STP 1), the year when the core was recovered. The other tie point was assigned to the depth of 868 cm with an age of 11,650 a BP (STP 2), reflecting the Pleistocene/Holocene boundary (Walker et al., 2012). The modelling was carried out through the following two steps. First, given the fact that the uppermost date (LU-10199) at 248 cm is a conventional date with significant dating uncertainties, we ran a first Bayesian chronological model from 248 to 885 cm, incorporating all ^{14}C dates, to extract more precise a median age for the depth 248 cm. Second, this age constraint was used along with the other ^{14}C dates and STPs to create a full chronological framework for the entire sequence.

3.3. Palynological analysis and visualisation of results

A total of 97 sediment samples (each representing a 2-cm layer) selected for palynological analysis were taken from RZ19. Palynomorphs were extracted using standard laboratory techniques applied to lacustrine and peat sediments (Fægri and Iversen, 1989; Krikunova et al., 2022). One tablet with a known number of *Lycopodium* spores was added to each sample prior to chemical treatment in order to calculate pollen concentration (PC, Stockmarr, 1971) and pollen accumulation rate (PAR, Knight et al., 2022). Pollen and spores were counted using a light microscope at ×400 magnification and identified following published atlases (Bobrov et al., 1983; Kupriyanova and Aleshina, 1972, 1978; Moore et al., 1991; Savelieva et al., 2013; van Geel, 2001) and reference collections. The Tilia software package (version 1.7.16) for Windows (Grimm, 2011) was used for calculating relative taxa percentages and for drawing the pollen diagram. Percentages for all terrestrial pollen taxa were calculated based on the sum of arboreal

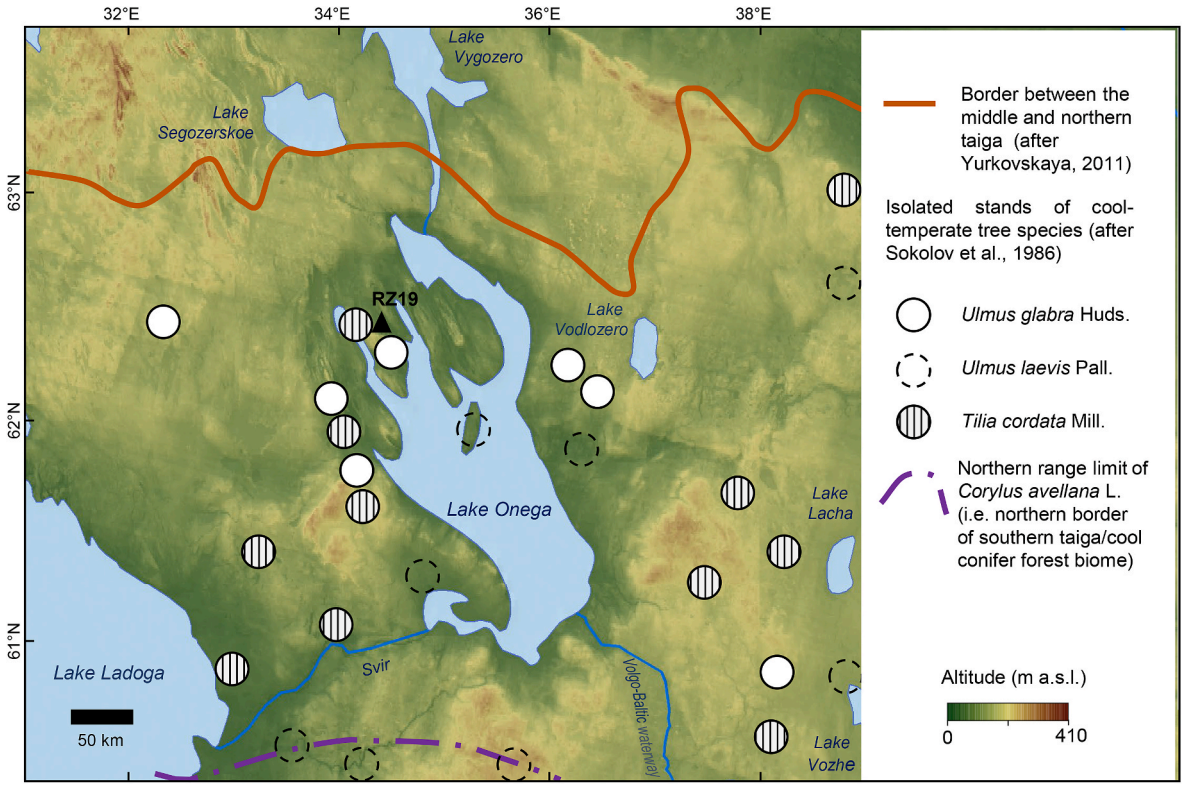

Fig. 2. Topographic map of the study region showing modern vegetation boundaries (after Yurkovskaya, 2011) and distribution of the thermophilic tree/shrub taxa discussed in the text (after Sokolov et al., 1986).

Table 2
Available ^{14}C dating results obtained on bulk sediments from the RZ19 sediment sequence, in addition to their calibrated and modelled ages in 95% probabilistic range and median. The^{14}C dates were calibrated in OxCal v.4.4 software (Bronk Ramsey, 1995) using the IntCal20 calibration curve (Reimer et al., 2020).

Laboratory code	Dated level (cm below core top)	^{14}C date (^{14}C yr BP)	Calibrated age, 95% range (a BP)	Calibrated age, median (a BP)	Modelled age, 95% range (a BP)	Modelled age, median (a BP)
LU-10199	248	2340 ± 150	2745–2003	2393	2697–2685	2692
Poz-139758	355.5	4760 ± 35	5586–5330	5519	5569–5326	5370
Poz-141040	439.5	6060 ± 35	7148–6794	6911	6945–6754	6820
LU-10200	446	6760 ± 310	8308–6995	7634	7009–6792	6887
Poz-140073	520.5	6400 ± 40	7424–7184	7325	7458–7304	7397
Poz-141041	578.5	7350 ± 40	8313–8026	8127	8198–8032	8092
LU-10201	610	8050 ± 300	9662–8214	8957	8530–8389	8446
Poz-141042	610.5	7660 ± 35	8538–8388	8443	8536–8394	8453
Poz-140075	665.5	8840 ± 40	10154–9711	9929	9573–9154	9393
Poz-140076	681.5	8810 ± 50	10153–9609	9849	9853–9561	9717

pollen (AP) and non-arboreal pollen (NAP) taken as 100%. Percentages for aquatic plant pollen and terrestrial cryptogams were calculated based on the terrestrial pollen sum plus the sum of palynomorphs in the corresponding group. The CONISS program (integrated into the Tilia software) for stratigraphically constrained cluster analysis by the method of incremental sum of squares (Grimm, 1987) facilitated the drawing of pollen zone boundaries.

3.4. Biome score calculation

Pollen-based vegetation reconstructions, using a quantitative approach known as the biomization technique, allows an objective and holistic interpretation of pollen data (e.g. Prentice and Webb III, 1998) and facilitates comparison with climate and vegetation modelling results (e.g. Kageyama et al., 2001; Prentice et al., 1996). The robustness of the method was tested using representative reference datasets of modern pollen spectra from Europe (Prentice et al., 1996) and other parts of extratropical Eurasia (e.g. Edwards et al., 2000; Mokhova et al., 2009; Sun et al., 2020; Tarasov et al., 1998). These successful tests allowed to apply the method to last glacial–interglacial pollen records in order to reconstruct spatiotemporal vegetation dynamics on a site (e.g. Wohlfarth et al., 2004), regional (e.g. Binney et al., 2017) and global scale (e.g. Wanner et al., 2008).

In the current study, all terrestrial pollen taxa identified in the Razlomnoe Peat record were assigned to their corresponding plant functional types (PFTs) and biomes (Table 3) following the biome-taxon matrixes presented in recent publications reconstructing Lateglacial-Holocene vegetation dynamics in the areas north (Krikunova et al., 2022) and south (Tarasov et al., 2022) of Lake Onega. The affinity scores for the natural potential biomes were calculated using an equation first published in Prentice et al. (1996). Landscape openness was assessed as the difference between the maximum forest biome score and the maximum open biome score calculated for each analysed spectrum (Tarasov et al., 2013).

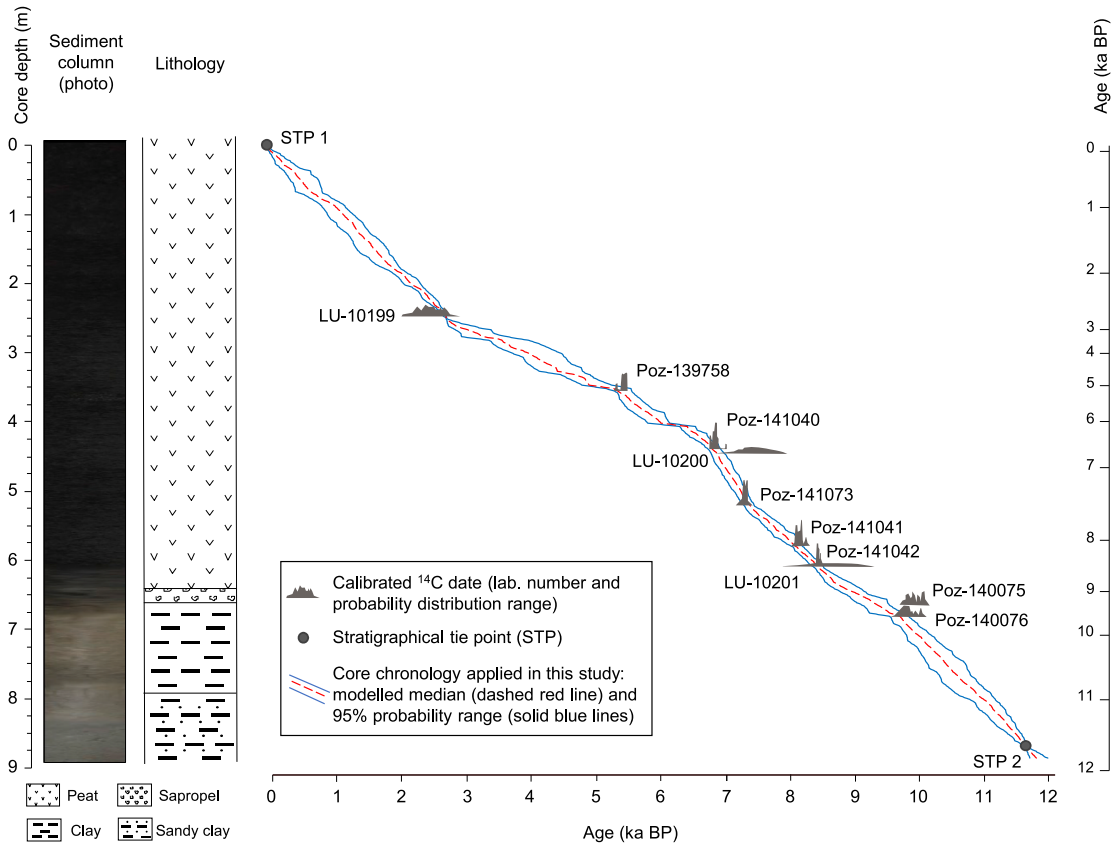

Fig. 3. Sediment column, schematic lithology and constructed age-depth model for the RZ19 sediment sequence discussed in this study. The two stratigraphical tie points are: −69 a BP at 0 cm (STP 1) and 11,650 a BP at 868 cm (STP 2).

4. Results

4.1. Sediment lithology and age determination

The RZ19 sediment core consists of four main lithological units (Fig. 3). The upper 641-cm unit is represented by dark-brown peat, poorly decomposed and heavily watered in the uppermost part (0–243 cm) and medium to well-decomposed in the lower part. This unit is underlain by a layer of grey-olive sapropel (641–663 cm), the clay content of which increases towards the base. The bottom part of the core is represented by grey-blue clay (663–781 cm), underlain by a clay unit with interlayers of fine-grained sand (781–885 cm). The transition from the lacustrine to the marsh phase in the core is recorded at a depth of 641 cm with a change from grey-olive sapropel to peat accumulation.

The age-depth model for the studied core (Fig. 3) underpins the interpretation of the palaeoenvironmental data. The model assigned an age of ca. 11.81 ka BP to the bottom of the core at 885 cm. Although in some sections the sedimentation rate shows small deviations from the average value (i.e. 1 cm in 13 years), no obvious depositional hiatuses can be detected.

4.2. Fossil pollen assemblages

The results of the palynological analysis are shown in Fig. 4. The entire record has been divided into eight local pollen assemblage zones (PAZs) numbered consequently from bottom to top (i.e. RZ19-1 to RZ19-8). To facilitate further discussion, the key features of the PAZs are summarised in Table 4 starting from the bottom/oldest one.

4.3. Reconstructed biomes and landscape openness

The results of the pollen-based biome (Fig. 5a and b) and landscape openness (Fig. 5c) reconstruction indicate a predominantly open landscape below 849 cm (before ca. 11,500 a BP), represented by cold grass-shrub communities attributed to the steppe (STEP) and tundra (TUND) biomes (Fig. 5b). The early afforestation phase (ca. 11,500–9000 a BP) began with the spread of boreal trees, representing cold deciduous (CLDE) and taiga (TAIG) forests, in which boreal evergreen conifers (bec), such as *Picea*, played a minor role (Fig. 5d). Several times during this interval, the cool conifer forest (COCO) biome has a slightly higher score than CLDE/TAIG, due to a very minor contribution of cool-temperate summer green (ts1) taxa, such as *Corylus* and *Ulmus* (Fig. 5d). The scores of TUND remain relatively high (Fig. 5a).

The phase between ca. 9000 and 6000 a BP shows predominance of the COCO biome score over the TAIG score, except during a short interval ca. 7500–7250 a BP (Fig. 5b). The cool mixed forest (COMX) biome is reconstructed two times (ca. 7990 and 6540 a BP), reflecting contribution of temperate summer green (ts) taxa, such as *Quercus*, and a generally high content of ts1 taxa (Fig. 5d). The reconstruction demonstrates the lowest scores of open vegetation types (TUND and STEP) and suggests a well-forested landscape (Fig. 5c) during this phase.

After ca. 6000 a BP, the biome reconstruction (Fig. 5b) shows a return to the co-dominance of the TAIG and COCO biomes, reflecting the largest contribution of bec taxa to the pollen assemblage and the temporary increasing role of ts1 taxa (Fig. 5d). The reconstruction (Fig. 5c) shows a trend towards a more open landscape and a spread of grass-shrub communities. A particularly noticeable shift in landscape openness is reconstructed around 4000 a BP.

The interval between ca. 1650 a BP and today shows the dominance of the TAIG biome (Fig. 5b), which reflects the insignificant role of temperate tree and shrub taxa in the regional forests (Fig. 5d). The reconstruction of COMX (Fig. 5b) at ca. 1140 a BP is obtained for one sample with a very low pollen concentration (and counts), which, as a result, enhances the role of a single grain of *Quercus*. The landscape

Table 3
Terrestrial pollen taxa identified in the RZ19 pollen record from Razlomnoe Peat (Fig. 5) and their assignments to plant functional types (PFTs) and regional biomes (after Tarasov et al., 1998). Only taxa which exceed the 0.5% universal threshold (Prentice et al., 1996) and therefore influence the calculation of biome score are included. Tc – temperature of the coldest month (°C), GDD5 – growing degree days above 5 °C, α – moisture index (after Prentice et al., 1996).

Plant functional types	Taxa from RZ19 included	Tc range	Min GDD5	Min α	Regional biomes
Arctic-alpine dwarf shrub (aa)	*Alnus fruticosa*, *Betula* sect. *Nanae/Fruticosae*			0.33	Tundra (TUND)
Arctic-alpine/boreal/ temperate summer green (aa/bs/ts)	*Salix*				TUND, Cold deciduous forest (CLDE), Taiga (TAIG), Cool conifer forest (COCO), Cool mixed forest (COMX)
Boreal evergreen conifer (bec)	*Picea*	−35 to −2	350	0.75	TAIG, COCO, COMX
Boreal summer green tree (bs)	*Betula* sect. *Albae*	<5	350	0.65	CLDE, TAIG, COCO, COMX
Boreal/temperate summer green tree (bs/ts)	*Alnus* (tree)				CLDE, TAIG, COCO, COMX
Eurythermic conifer (ec)	*Pinus sylvestris/P. Diploxylon*	> −35	350	0.65	CLDE, TAIG, COCO, COMX
Cool-temperate summer green (ts1)	*Corylus, Frangula, Tilia, Ulmus*	−15 to 10	900	0.65	COCO, COMX
Temperate summer green (ts)	*Quercus* (deciduous)	−15 to 15.5	1200	0.65	COMX
Grass (g)	Poaceae				TUND, steppe (STEP)
Heath (h)	Ericales			0.65	TUND, CLDE, TAIG, COCO, COMX
Sedge (s)	Cyperaceae		500	0.20	TUND
Steppe forb (sf)	Apiaceae, Asteraceae (subfam. Asteroideae, Cichorioideae), Brassicaceae, *Cannabis,* Caryophyllaceae, Lamiaceae, Liliaceae, Ranunculaceae, Rosaceae (*Filipendula, Potentilla)*				STEP
Steppe/desert forb (sf/df)	*Artemisia*, Chenopodiaceae				STEP, desert (DESE)
Desert forb (df)	*Ephedra*		500		DESE
Arctic-alpine/steppe/desert forb (aa/sf/df)	Polygonaceae				TUND, STEP, DESE

openness continues to be relatively high, particularly between ca. 680 and 380 a BP, while forest spread is reconstructed for the 1990s.

5. Discussion

5.1. The Lateglacial

The Lateglacial pollen assemblage in RZ19 represents the end phase of the Younger Dryas (YD), ca. 11,810–11,650 a BP. High proportions of herbaceous taxa (56–60%) and birch shrubs (Fig. 4), along with low PC and PAR values, indicate a predominantly open landscape with tundra-steppe vegetation. The highest percentages of wormwood (13–17%) and chenopods (up to 12.5%), known for their wide adaptability, reflect disturbed grounds and aridity of the YD climate in the region. Quantitative biome reconstruction supports this interpretation, demonstrating the highest scores for the cold steppe and shrub tundra biomes (Fig. 5a). The very robust chronology of a multiproxy environmental archive from Lake Pichozero (Fig. 1b), constrained by varve counting and AMS ^{14}C ages of terrestrial plant macrofossils (Wohlfarth et al., 2004), covers the period from 12,800 to 9300 a BP and allows a direct comparison with RZ19. The two records show very similar pollen composition and low PCs up to ca. 11,650 a BP, but the contribution of NAP taxa is somewhat smaller in Lake Pichozero, possibly due to its more southern location, about 170 km southeast of Razlomnoe Peat.

Consistent with the results of the current study (Table 4), low PCs and relatively high percentages of NAP taxa in poorly dated sediments assigned to the YD allowed the reconstruction of herbaceous and shrub-moss tundra with the participation of steppe and halophyte elements in the regional mosaic vegetation (e.g. Velichko et al., 2017). Robustly dated records from Pichozero and Tambichozero (Fig. 1b; Wohlfarth et al., 2002, 2004) also suggest a cold and dry climate with predominantly tundra vegetation evidenced by macrofossil finds of *Betula nana* and *Dryas octopetala*. While there is general agreement on the generally open YD landscape, there is no consensus on the presence/absence of trees. Velichko et al. (2017) suggested the presence of birch trees, juniper and *Hippophae* shrubs near Lake Onega, however, the macrofossil records from Tambichozero (Wohlfarth et al., 2002) and Pichozero (Wohlfarth et al., 2004) do not reveal remains of *Betula pubescens* during the YD. Although, several published pollen records from the LOR demonstrate noticeable amounts of *Betula* sect. *Albae* pollen, which is often regarded to have been reworked or wind-transported. In the absence of directly dated tree or erect shrub macrofossils, the question remains open. However, very rapid afforestation of the area around Lake Onega in the Early Holocene, as suggested by the RZ19 pollen record and some earlier studies (e.g. Binney et al., 2017; Kremenetski et al., 1998; Velichko et al., 2017; Wohlfarth et al., 2007), as well as the macrofossil-confirmed growth of boreal trees in even colder parts of Northern Eurasia during the YD (e.g. Binney et al., 2009; Werner et al., 2010), may indicate the presence of scattered trees in the most favourable wind-protected and moist environments.

Abraham et al. (2021), using patterns in recent PARs across Europe as a tool for vegetation reconstruction, demonstrated that (i) at least 140 grains/cm^2/a of tree pollen may be found in a treeless landscape and (ii) with each 10% of forest cover, tree PAR increases by at least 400 grains/cm^2/a. Thus, average PAR values for terrestrial (1270 grains/cm^2/a) and tree taxa (208 grains/cm^2/a) in the Lateglacial part of the RZ19 record (Table 4 and Fig. 5e) support rather open, although not completely treeless vegetation in the study area.

5.2. The Early Holocene (Greenlandian)

Between 11,650 and 8280 a BP, the RZ19 record shows rapid changes in pollen composition (Fig. 6a) and vegetation cover (Fig. 6b), reflecting the temperature shift from the YD cold phase to the Holocene well-documented in the Greenland ice cores and in other key global climate archives (e.g. Nakagawa et al., 2021; Svensson et al., 2008; Walker et al., 2012). The increase in arboreal pollen from 12.5 to 71.4% between ca. 11.7 and 11.3 ka BP (Fig. 5a) reflects an increase in NGRIP δ^{18}O values (Fig. 6c) and a reconstructed increase of the mean annual temperature by ~7 °C (Fig. 6d). The biome reconstruction (Fig. 5a) suggests rapid afforestation of the area surrounding the RZ19 site in the Early Holocene, although the scores of the tundra biome remain

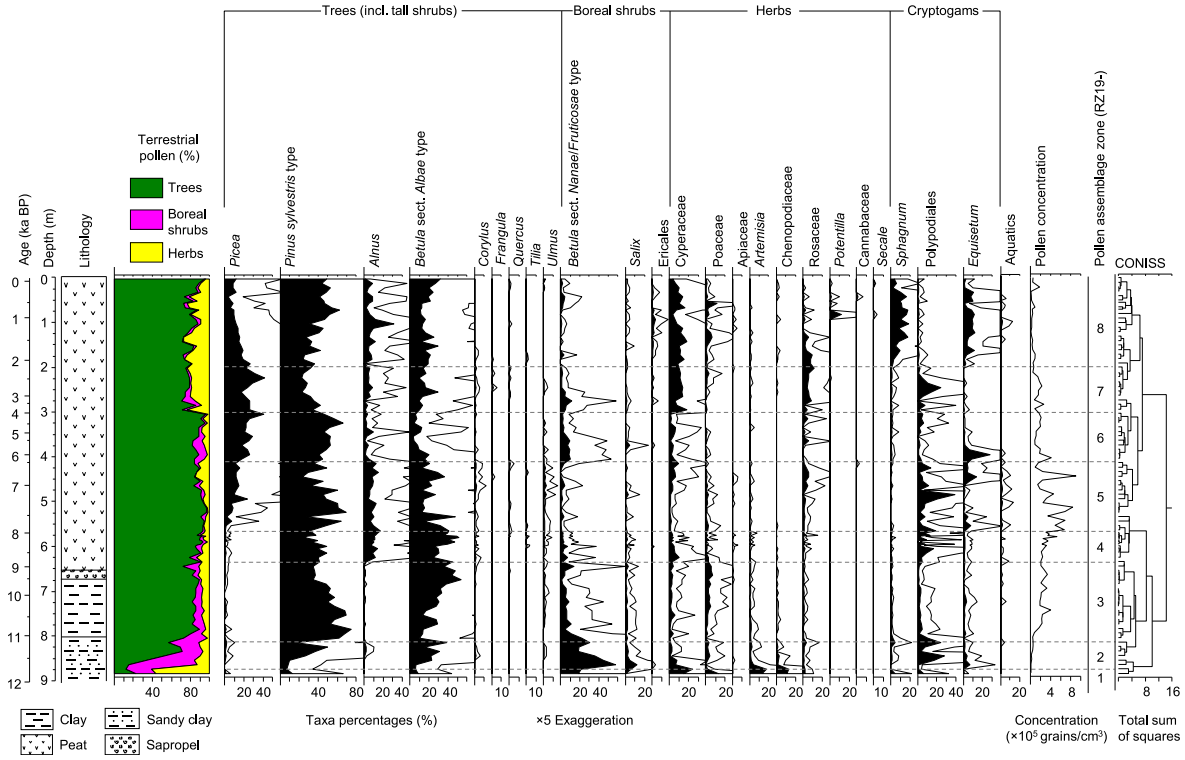

Fig. 4. Simplified percentage diagram of the RZ19 record showing arboreal and non-arboreal pollen taxa and terrestrial cryptogams plotted against the core depth and age axes. Dashed horizontal lines indicate pollen assemblage zone (PAZ) boundaries.

relatively high and the vegetation was likely more open than today before ca. 9000 a BP (Fig. 6b). The relatively low PC and PAR values, as well as the relatively high NAP percentages in the RZ19 record (Table 4) confirm previous studies (Filimonova and Lavrova, 2015; Lavrova, 2005; Saarnisto et al., 1995), which concluded that tundra communities still played an important role in the earliest Holocene landscape (ca. 11, 650–9900 a BP), along with birch and pine-birch forests similar in appearance to northern taiga.

Although a few pollen grains of elm and hazel were found in subsamples of the RZ19 sediment core as old as ca. 11,400–11,300 a BP (Fig. 4), they probably represent long-distance wind transport superimposed on low pollen concentrations. However, long-distance transport is unlikely to explain high pollen percentages of other arboreal taxa, such as birch and Scots pine. The rise in *Betula* sect. *Albae* percentages and concentrations in RZ19 (Fig. 4) coincides with the first appearance of *B. pubescens* and *P. tremula* macrofossils in the Pichozero record at ca. 11,500 a BP (Wohlfarth et al., 2004) and indicates that both tree species were growing in the LOR at that time.

Immigration and spread of spruce in the LOR are other frequently debated topics (e.g. Elina et al., 2010; Savelieva, 2010), although their study is hampered by the lack of reliable chronologies (Giesecke and Bennett, 2004). In the RZ19 pollen record (Fig. 4), the percentage of *Picea* remains low throughout the Early Holocene interval until ca. 8150 a BP. Plant macrofossils manifested growth of *Picea abies* at Pichozero ca. 10,750 and 10,000 a BP (Wohlfarth et al., 2004) when the percentages of *Picea* pollen did not exceed 5%. However, similar or even higher *Picea* percentage and concentration values are recorded at Pichozero and Tambichozero from about 11,500 a BP (Wohlfarth et al., 2002, 2004). The records of vegetation from the sites around Lake Onega suggest that, although the participation of spruce in the canopy was minimal, it participated in the colonisation of tundra soils by forests dominated by birch and pine since the beginning of the Holocene.

Another notable feature of the Early Holocene pollen assemblage in the RZ19 record is the marked increase in the proportion of *Alnus* after ca. 9000 a BP (Fig. 4), indicating a major spread of alder in the study area. Particularly, grey alder (*A. incana*), a fast-growing pioneer tree or a multi-stemmed shrub, is extremely frost-tolerant and can be found up to the tree line in parts of northern Europe (Houston Durrant et al., 2016). From about the same time, *Corylus* pollen regularly appears in the record and percentages of *Betula* sect. *Nanae/Fruticosae* continue to decrease, indicating further warming of the regional climate and migration of hazel north and east of its modern distribution range (Fig. 2). This is supported by the pollen data from Pichozero, where *Corylus* may have been present as early as 9600 a BP (Wohlfarth et al., 2004). Both grey and common alder (*A. glutinosa*) are able to fix nitrogen in symbiotic root nodules, making it useful for improving soil condition (Houston Durrant et al., 2016). The almost synchronous appearance of *Alnus* and *Corylus* at Razlomnoe could also indicate the maturation of soils.

5.3. The Middle Holocene (Northgrippian)

The Middle Holocene (ca. 8280–4200 a BP) in the RZ19 record is characterised by an increase in pollen productivity (maximum PC and PAR values) and a progressive expansion of *Picea* (Fig. 4). The highest AP percentages (Fig. 6a) and reconstructed landscape openness (Fig. 6b) suggest further afforestation of the area reaching a maximum about 7350 a BP. The Middle Holocene interval is also characterised by the highest diversity and abundance of thermophilic summer green tree-shrub taxa (i.e. ts, ts1, Table 3), which helps to explain the frequent reconstruction of cool conifer (i.e. southern taiga) and cool mixed forest biomes (Fig. 5b). The results from RZ19 reflect optimal conditions for species-rich pine-spruce-birch forests, with temperate elements such as hazel, elm, linden and oak extending beyond their modern ranges. The ^{14}C-dated pollen record from Sambalskoe (Elina et al., 2010, Fig. 1b) on the western shore of Lake Onega about 80 km south of RZ19 demonstrates the dominance of spruce-pine-birch forests with an even higher admixture of thermophilic taxa after ca. 8000 a BP. According to both records, the maximum contribution of warm-loving trees and shrubs, reflecting the Holocene thermal maximum in the LOR, occurred in the first half of the Middle Holocene, followed by an interval of cooler

Table 4
Characteristics of pollen assemblage zones (PAZs) in the RZ19 sediment sequence, including their modelled ages in calibrated a BP (95% probabilistic ranges and medians).

Pollen assemblage zone (cm)	Modelled age, 95% range and *median* (a BP)	PAZ: Dominant taxa and characteristic features, including average pollen concentrations (PC, grains/cm^3) and pollen accumulation rates (PAR, grains/cm^2/a)
RZ19-1 (885–869)	11,987/11,707–11,672/11,649; *11,810–11,660*	**Cyperaceae–*Betula* sect. *Nanae/Fruticosae–Artemisia*–Chenopodiaceae** – Herbs and boreal shrubs predominate: Cyperaceae (14–24%), *Artemisia* (13–17%), Chenopodiaceae (11–13%) and Poaceae (2–13%), *Betula* sect. *Nanae/Fruticosae* (19–21%), *Salix* (up to 6%). *Betula* sect. *Albae* (6–9%) and *Pinus sylvestris* (7–13%) are at minimums. PC (10,060 grains/cm^3) and PAR (1270 grains/cm^2/a) averages are low.
RZ19-2 (869–809)	11,672/11,649–11,264/10,885; *11,660–11,100*	***B.* sect. *Nanae/Fruticosae–B.* sect. *Albae–Pinus–Salix*** – Pollen contribution from trees and boreal shrubs increases rapidly (84–93%). *B.* sect. *Nanae/Fruticosae* reaches maximum, with two peaks (57% and 30%). *Salix* shows maximum (12%) in the lower part, followed by a decrease to 0.8%. *P. sylvestris* reaches 50% and then drops to 16%. *B.* sect. *Albae* varies from 16 to 39%. Single grains of tree *Alnus*, *Corylus* and *Ulmus* appear from 844 cm (ca. 11,400 a BP). Peaks of Polypodiales (28%) and *Lycopodium clavatum* (7%). PC (31,730 grains/cm^3) and PAR (3635 grains/cm^2/a) averages increase.
RZ19-3 (809–629)	11,264/10,885–8888/8537; *11,100–8670*	***Pinus–B.* sect. *Albae–B.* sect. *Nanae*** – Increase in AP up to 90%. *P. sylvestris* reaches maximum (74%) in the lower part and *B.* sect. *Albae* (53%) in the upper part. *Ulmus* and *Corylus* appear more regularly, although in small amounts. Boreal shrubs (mainly *B.* sect. *Nanae/Fruticosae*) and herbs average about 7% and cryptogam spores average 5%. PC (221,810 grains/cm^3) and PAR (18,660 grains/cm^2/a) averages continue to increase.
RZ19-4 (629–567)	8888/8537–8103/7832; *8670–7960*	***B.* sect. *Albae–Pinus–Alnus*–Cyperaceae** – High values of *B.* sect. *Albae* (24–51%) and *P. sylvestris* (25–49%), rapid increase of tree *Alnus* (7–13%) and single occurrences of *Ulmus*, *Corylus*, *Tilia* and *Quercus*. Boreal shrubs do not exceed 8% and herbaceous taxa (mainly Cyperaceae and Poaceae) contribute 2–13%. Polypodiales reaches peak values of up to 17%. PC (308,810 grains/cm^3) and PAR (27,590 grains/cm^2/a) averages continue to increase.
RZ19-5 (567–409)	8103/7832–6561/6327; *7960–6440*	***Pinus–B.* sect. *Albae–Alnus–Picea*** – Absolute dominance of tree pollen (84–97%) mainly represented by *P. sylvestris* (24–69%) and *Betula* sect. *Albae* (up to 48%). *Picea* shows continuous presence and high percentages (up to 23%). *Alnus* remain relatively high (4–17%). Highest values (>2%) of *Ulmus* and *Corylus*. *Tilia*, *Quercus* and *Frangula alnus* appear discontinuously. The boreal shrubs and herbs account for an average of 2% and 6%. The cryptogams are dominated by Polypodiales and *Equisetum*. PC (435,920 grains/cm^3) and PAR (51,650 grains/cm^2/a) averages are highest in the record.
RZ19-6 (409–299)	6561/6327–4461/3717; *6440–3960*	***Pinus–Picea–B.* sect. *Albae–B.* sect. *Nanae/Fruticosae*** – AP taxa remain dominant (82–96%), with *P. sylvestris* (46–66%), *Picea* (up to 41%), *B.* sect. *Albae* (4–20%) and *Alnus* (1–10%). Temperate summer green taxa appear less frequently. *B.* sect. *Nanae/Fruticosae* (11%), *Salix* (5%) and *Equisetum* (up to 28%) show relatively high values in the lower part of this zone, while the contribution of herbs (2–8%) is minimal. Decreasing average values of PC (175,780 grains/cm^3) and PAR (8240 grains/cm^2/a).
RZ19-7 (299–187)	4461/3717–2283/2019; *3960–2130*	***Picea–Pinus–B.* sect. *Albae*–Cyperaceae** – Decrease in AP (70–85%). *Picea* reaches its maximum (42%). *P. sylvestris* decreases from 42% to 23%, followed by an increase to 32%. *B.* sect. *Albae* shows a peak (29%) in the middle part. *Alnus* remains below 9%. *Corylus*, *Frangula*, *Quercus* and *Ulmus* are rare, but *Tilia* disappears. Increase in NAP (8–23%), mainly in Cyperaceae (6–18%) and Rosaceae (up to 12%). *B.* sect. *Nanae/Fruticosae* shows a peak (12%) in the lower part of the PAZ. Peak in Polypodiales (24%), while *Equisetum* almost disappears. PC (125,710 grains/cm^3) continue to decrease and PAR (9145 grains/cm^2/a) remains relatively low.
RZ19-8 (187–0)	2283/2019– present; *2130–present*	***Pinus–B.* sect. *Albae–Picea–Alnus*** – AP contributes 71–95% and is highly variable. NAP (4–27%), mainly Cyperaceae, Poaceae, Rosaceae and *Potentilla*, changes in antiphase. *P. sylvestris* (24–62%), *Picea* (4–26%), *B.* sect. *Albae* (11–32%) and *Alnus* (1–32%) dominate. Pollen grains of *Corylus*, *Ulmus* and *Quercus* are rare. The high content of *Sphagnum* (up to 18%) and *Equisetum* (up to 12%) and first appearance of *Secale* (82.5 cm, 750 a BP) characterise this zone. PC decreases to 40,080 grains/cm^3 and PAR to 5305 grains/cm^2/a.

climate, which led to a noticeable increase in the share of spruce (Elina et al., 2010).

Reconstructing the spread of spruce in Fennoscandia using published pollen data and GIS analysis, Giesecke and Bennett (2004) estimated that the *Picea* pollen contribution around Lake Onega for the first time exceeded the 10% level between 7000 and 6000 a BP, while the maximum value was reached in the Late Holocene. This estimate, based on limited data from the region, is partly supported by the RZ19 record, where the percentage of *Picea* exceeds the 10% level after ca. 7200 a BP.

Growing pollen percentages of spruce in the RZ19 record from ca. 7950 a BP indicate a wider spread of this tree taxon in the vegetation. With a shallow root system well-adapted to moist, cool boreal and high-elevation environments, spruce is rather vulnerable to drought (Henne et al., 2011). Given that spruce appeared near Lake Onega already in the Early Holocene (e.g. Savelieva, 2010; Wohlfarth et al., 2004), its rapid spread in the Middle Holocene likely reflects wetter climate conditions, as evidenced by the higher moisture requirements of bec taxa in the BIOME global vegetation model based on plant physiology and dominance, soil properties and climate (Prentice et al., 1992).

5.4. The Late Holocene (Meghalayan)

The onset of the Late Holocene (ca. 4200 a BP to the present) in the RZ19 record (Fig. 6a) is marked by a sharp decrease in the amount of AP and a parallel increase in NAP (mainly Cyperaceae and Rosaceae) and fern spores (Fig. 4), which indicates an environmental shift towards more open vegetation (Fig. 6b). Without evidence of strong human impact (e.g. forest logging, slash and burn agriculture), such changes are often interpreted as the onset of drier conditions, which may be associated with warmer or colder climates. In our case, the reconstruction of the taiga biome (Fig. 5b) and the record-wide highest percentages of *Picea* point to cooling but speak against drying. The decrease in forest coverage in the study area is most likely due to excess moisture and waterlogging processes, as evidenced by studies of modern paludification and forest retreat in northern environments (Crawford et al., 2003) and supported by a gridded pollen-based precipitation reconstruction in Europe (Mauri et al., 2015). Higher values for Cyperaceae, Ericales, *Betula* sect. *Nanae/Fruticosae* pollen and Polypodiales spores support this interpretation (Mishra et al., 2016). A later increase in *Equisetum* and *Sphagnum* spores (Fig. 4) also indicates that the development of sphagnum-dominated bogs intensified after ca. 1900 a BP. The forests were dominated by pine, birch and alder trees, while participation of spruce decreased to the Middle Holocene level. Single grains of *Secale* (rye) pollen appear in RZ19 from ca. 750 a BP (Fig. 4). This is in agreement with Vuorela et al. (2001), who dated the start of land clearance for permanent cultivation to the late 13th century CE and the beginning of more intensive field cultivation to the 15th century CE at Pegrema (Fig. 1b), located ~20 km southeast of Razlomnoe.

5.5. Sensitivity of the RZ19 record to the 8.2 and 4.2 ka BP events

The lack of noticeable anthropogenic impact, the robust chronology,

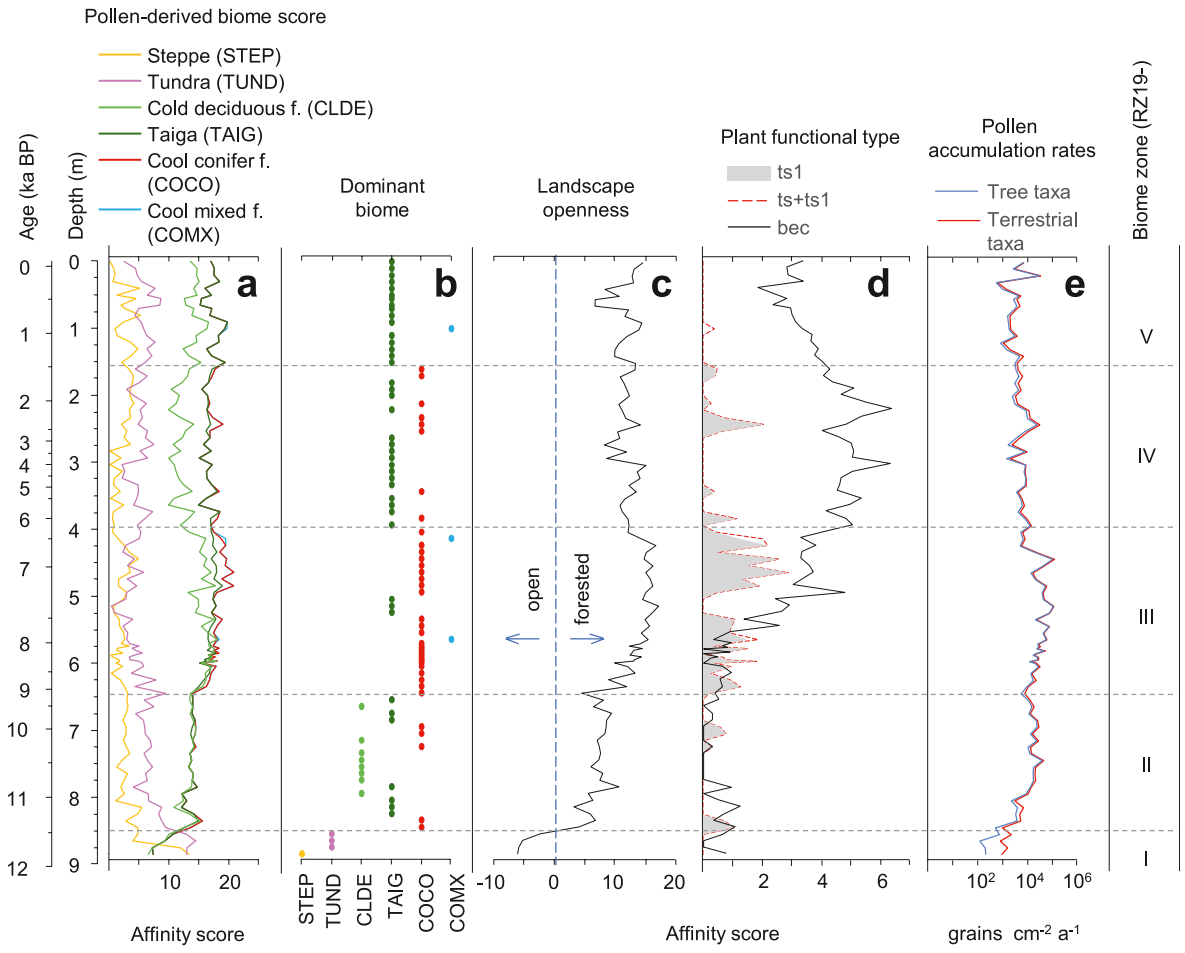

Fig. 5. Summary chart showing results of biome score calculation (a), biomes with the highest affinity score (b), reconstructed landscape openness (c), affinity scores (d) for selected climate-sensitive tree/shrub plant functional types (PFTs), including cool-temperate summer green (ts1), temperate summer green (ts), and boreal evergreen conifer (bec) PFT, as well as pollen accumulation rate (PAR) values (e), with the corresponding biome zones plotted against the core depth and age axes.

continuous sediment accumulation and fairly high sedimentation rates of on average 0.75 mm/a suggest that the RZ19 pollen record is a valuable archive of native vegetation, which in turn is the best expression of climate (Köppen, 1923) in the study region. The global vegetation model BIOME (Prentice et al., 1992) utilises this concept of W. Köppen and provides a way to interpret the relative changes in the PFT scores based on a well-defined limited set of bioclimatic variables (Table 3). Thus, the distribution of bec (see Table 3 for detail), including *Picea*, reflects an increase in the moisture index (expressed as the ratio of actual to equilibrium evapotranspiration) above 0.75, and the distribution of temperate summer green (ts1 and ts) taxa (Fig. 5d) reflects an increase in the mean temperature of the coldest month above −15 °C and in the annual sum of daytime temperatures above 5 °C (GDD5) above 900 and 1200, respectively (Prentice et al., 1996). Although, the interpretation of the record regarding temperature and precipitation dynamics can be complicated by internal processes of landscape and vegetation evolution, the general trends and secular variations in pollen percentage (Fig. 6a) and landscape openness values (Fig. 6b) reflect well (within the accuracy of the age model) the insolation-induced temperature changes in the ice core record from Greenland (Fig. 6c) and in the proxy-based reconstructions from Finland (Fig. 6d and e). By demonstrating a temporal coincidence of the pollen/vegetation shifts in RZ19 with the global climate shifts across the Greenlandian-Northgrippian and Northgrippian-Meghalayan transitions (Fig. 6), the current study provides environmental support for the formal three-part division of the Holocene in the region around Lake Onega. However, the hypothesis put forward by Wohlfarth et al. (2004) on the basis of the Pichozero record of the Lateglacial-Holocene transition that even relatively minor century-scale climate signals from the Holocene are detectable in the study region needs to be further tested.

The 8.2 and 4.2 ka BP events represent two of the most extensively documented rapid climate changes of the Holocene, marking the transitions between the Greenlandian and Northgrippian (Early to Middle Holocene) stages and between the Northgrippian and Meghalayan (Middle to Late Holocene) stages, respectively (Magny et al., 2013; Walker et al., 2012, 2018). The abrupt 8.2 ka BP cooling lasted for two to four centuries and was supposedly triggered by a massive freshwater outburst from the glacial Lake Agassiz-Ojibway (Alley et al., 1997; Rohling and Pälike, 2005). The cooling is well-recognised in $\delta^{18}O$ and temperature records from Greenland ice cores (Fig. 6c and d) and coincides with an interval of weaker East Asian (e.g. Tan et al., 2020) and Indian (e.g. Dixit et al., 2014b) summer monsoon. While the temperature reconstruction for Greenland (Fig. 6d) shows a distinct drop in mean annual temperature of 3.5 °C centred around 8160 a BP, published records from eastern Fennoscandia are less conclusive in terms of timing and magnitude of cooling (e.g. Eräsẗo et al., 2012, Fig. 6f), which can be partially explained by the problems of the respective age models and the different climatic sensitivity of the studied sites and proxies (e.g. Parker and Harrison, 2022).

To date, there is no published environmental evidence of the 8.2 ka BP event from the LOR and the suggested climate scenario (Filimonova and Lavrova, 2017) shows higher than present mean annual temperatures and precipitation between 8.5 and 8.0 ka BP. The mean annual air temperature reconstruction from Lake Laihalampi, southern Finland

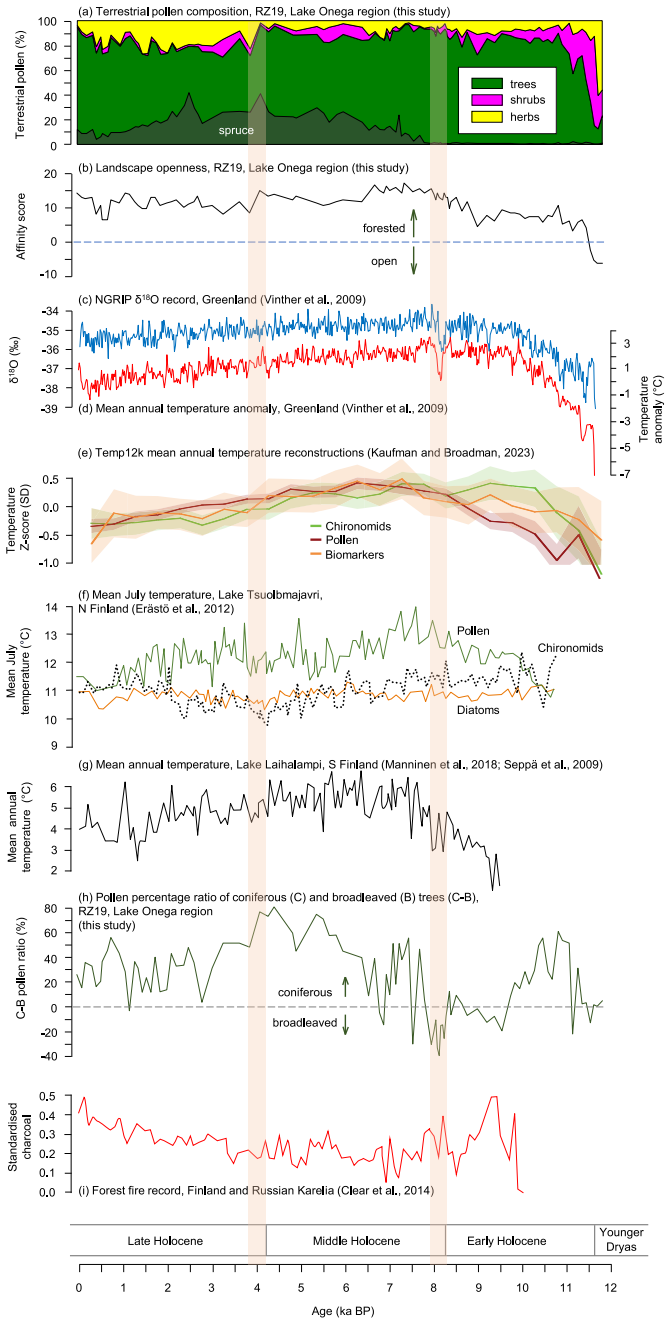

Fig. 6. Summary chart showing (a) terrestrial pollen composition and (b) landscape openness derived from the RZ19 pollen record, Lake Onega region (this study); (c) NGRIP $\delta^{18}O$ record, Greenland and (d) mean annual temperature anomaly, Greenland (after Vinther et al., 2009); (e) composites for terrestrial proxy types (i.e. pollen, chironomids and biomarkers) from the Temp12k global database of Holocene palaeotemperature records (after Kaufman and Broadman, 2023); (f) proxy-based mean July temperature reconstructions, Lake Tsuolbmajavri, Finnland (after Eråstö et al., 2012); (g) pollen-derived mean annual temperature, Lake Laihalampi, Finland (after Manninen et al., 2018; Seppä et al., 2009); (h) pollen percentage ratio of coniferous (C) and broadleaved (B) trees (C – B), RZ19, Lake Onega region (this study); and (i) forest fire record, Finland and Russian Karelia (after Clear et al., 2014). Vertical stripes highlight the intervals of 8300–8100 and 4200–3800 a BP, corresponding to the Early-Middle and Middle-Late Holocene transitions, respectively.

(Fig. 6g), displays two minimums, with a relative temperature decrease of up to 2 °C (Manninen et al., 2018; Seppä et al., 2009). In contrast, a robustly dated archaeological record from Yuzhniy Oleniy Ostrov (YOO), a small island in Lake Onega (Fig. 1b), located ca. 65 km southeast of RZ19 and famous for its large Late Mesolithic burial ground, demonstrates the main use of the cemetery ca. 8250–8000 a BP, which coincides remarkably well with the 8.2 ka BP cooling event (Schulting et al., 2022). The age model and resolution of the RZ19 record provide an opportunity to fill a gap in current knowledge and assess the environmental impact of the cooling event.

The RZ19 record (Fig. 4) shows a very weak decrease in AP, but no pollen of temperate deciduous taxa, except for three *Ulmus* grains in the sample dated to ca. 8186 a BP, a decrease in arboreal *Alnus* percentages and very low values or absence of *Picea* ca. 8300–8000 a BP. In contrast, *Betula* sect. *Albae* shows a marked increase in pollen percentage (with a peak value ca. 8150 a BP), while *P. sylvestris* experiences a marked decrease. This change in riparian vegetation, with birch dispersal at the expense of pine between 8300 and 8000 a BP, the most prominent of the entire record (Fig. 6h), likely made the habitats near Lake Onega more attractive to large game such as Eurasian elk and reindeer, remains of which were found in the YOO burials (Schulting et al., 2022). Similar ecotonal changes, as indicated by the *Pinus/Betula* pollen ratio, are observed in the pollen records further north (Allen et al., 2007; Manninen et al., 2018) and west of Lake Onega (Elina et al., 2010). Intensified wildfires (Fig. 6i) can be particularly dangerous in dry pine forests and may be another reason for the concentration of animals and people around a large lake as suggested by Schulting et al. (2022).

The above changes in the landscape can be explained by severe winter cooling and dry continental climate with relatively low precipitation and thin snow cover associated with the impact of the 8.2 ka BP event in the North Atlantic region (Li et al., 2019; Matero et al., 2017; Wiersma and Renssen, 2006). The normal development of Scots pine requires summer thawing of the active layer down to a depth of 1.5–2 m (Parfenova et al., 2021). One can speculate that strong winter cooling in combination with wildfires created less favourable conditions for the reproduction and spread of pine, while the fast-growing birch occupying moist habitats benefited most from this situation. Pollen-based reconstructions through a synthesis of palynological data from northern Europe show no or weak evidence for colder summer temperatures and suggest that cooling took place mostly during winter and spring (Seppä et al., 2007, 2009). Newer studies from Ireland (Ghilardi and O'Connell, 2013), Poland (Filoc et al., 2017) and Norway (Paus et al., 2019) indicate that summer temperature depression is also included and results in reduced pollen production. Consequently, European forest ecosystems responded sensitively to the cooling during the onset of the growing season, as documented by a marked decrease in temperate deciduous broadleaved trees across the region (Li et al., 2019; Magny et al., 2013; Seppä et al., 2007). In particular, the decline of *Alnus* (likely *A. glutinosa* highly sensitive to frost damage) in a high-resolution pollen record from Estonia was interpreted as evidence of particularly cold conditions in the area associated with the 8.2 ka BP event (Veski et al., 2004).

The 4.2 ka BP event, considered the beginning of the Meghalayan age (Head, 2019), is often cited as one of the most severe drought events of the Holocene (DeMenocal, 2001; Dixit et al., 2014a; Roland et al., 2014; Walker et al., 2012), although its exact cause remains poorly understood (Wanner et al., 2008). The event has not received attention in palaeoenvironmental studies focused on the LOR (Elina et al., 2010; Filimonova and Lavrova, 2017; Nazarova et al., 2020). However, the interval ca. 4200–3800 a BP (Fig. 6) in the RZ19 record demonstrates distinct shifts in the AP/NAP percentage (Fig. 6a) and landscape openness (Fig. 6b) that separate the more forested Middle Holocene landscape from the more open Late Holocene. The *Picea* (40.7%) and *Alnus* (3.6%) pollen proportions show well-recognised maxima about 4070 a BP. The coniferous taxa pollen percentage sum peaks at ca. 4600–4000 a BP, followed by a stepwise increase in the content of cold tolerant broadleaved trees, mainly represented by *Betula* sect. *Albae* (Fig. 6h). The scarce presence of thermophilic taxa and a minimum in PC along with a peak in NAP is registered at 3850 a BP (Fig. 4). The changes in RZ19 between ca. 4200 and 3800 a BP correspond to an oscillation

towards cooler annual temperature in the record from Lake Laihalampi (Fig. 6g) with a minimum at ca. 3850 a BP. The July temperature curves reconstructed from the multiproxy record of Lake Tsuolbmajavri (Fig. 6f) show minimum values at 4250 a BP (chironomids and diatoms) and 3850 a BP (pollen), which may reflect a different sensitivity of aquatic and terrestrial proxies to the climate change.

Despite the lower resolution, the RZ19 record shows fairly good agreement with short-term temperature variability superimposed on the hemispheric cooling trend observed in the Greenland record (Fig. 6d) and in global proxy-based reconstructions (Kaufman and Broadman, 2023, Fig. 6e). However, its pollen composition does not indicate a dry event around 4000 a BP. Higher values for Cyperaceae, Ericales, *Betula* sect. *Nanae/Fruticosae* pollen and Polypodiales spores are more likely to reflect a very wet environment and a waterlogged area (e.g. Mishra et al., 2016). A forest fire record from Finland and Karelia (Fig. 6i) also shows a relative decrease in fire activity, which does not indicate a drier environment.

6. Conclusions

The sediment core RZ19 provides a new continuous pollen and vegetation record of the last ca. 11.8 ka BP. The combination of the core length/age, sedimentation continuity, robust chronology and centennial resolution of the record is unique for the LOR and allows for (i) objective reconstruction of changes in land cover and forest composition; (ii) assessing the sensitivity of regional vegetation to climate dynamics in the Northern Atlantic; and (iii) checking the vegetation responses to the 8.2 ka and 4.2 ka BP events used to formally subdivide the Holocene epoch.

The results of the pollen analysis and quantitative pollen-based biome reconstruction show rapid afforestation of the area in the Early Holocene, although the scores of the tundra biome remain relatively high, suggesting that the vegetation was likely more open than today before ca. 9000 a BP. The marked increase in the proportion of tree alder occurs after ca. 9000 a BP, and *Corylus* pollen regularly appears in the record from about the same time, indicating further warming of the regional climate, soil maturation and migration of hazel north and east of its modern distribution range.

The main features of the Middle Holocene include the highest percentages and concentrations of arboreal pollen and the highest diversity and abundance of thermophilic summer green tree-shrub taxa in the entire RZ19 record, which explains the reconstruction of the cool conifer forest biome around the site. Growing pollen percentages of *Picea* from ca. 8000 a BP indicate a wider spread of spruce in the vegetation north of Lake Onega and reflect wetter climate conditions, as evidenced by the higher moisture requirements of this taxon in the BIOME vegetation models.

The decrease in arboreal and *Picea* pollen percentages and the parallel increase in landscape openness after ca. 4000 a BP likely reflect the combined effect of insolation-induced temperature decrease and associated paludification causing forest retreat rather than a decrease in atmospheric precipitation and/or spread of Late Neolithic agriculture. The appearance of rye pollen grains starting ca. 750 a BP is consistent with the start of land clearance for permanent cultivation in the late 13th century CE, as documented in earlier studies.

The results of pollen analysis and the pollen-based biome reconstruction demonstrate distinct changes in the vegetation cover and composition at the YD-Greenlandian, Greenlandian-Northgrippian and Northgrippian-Meghalayan boundaries, which confirms high sensitivity of the regional vegetation to hemispheric-scale climate dynamics suggested earlier for the Lateglacial-Holocene transition and allows to extend this assumption to the entire Holocene epoch.

Our study provides the first convincing evidence of a strong environmental impact from the 8.2 ka BP event in the study area, with the dispersal of birch at the expense of pine (the most prominent shift of this kind during the entire Holocene) and the reduction of alder (likely *A. glutinosa*) and other temperate deciduous taxa in the regional forests between 8300 and 8000 a BP. This distinct change in vegetation composition, peaking around 8200–8150 a BP, can be explained by severe winter and spring cooling, low precipitation and thin snow cover, and the high frequency of forest fires reconstructed by earlier studies.

The RZ19 record also shows marked pollen percentage oscillations and shifts in vegetation ca. 4200–3800 a BP, which can be associated with the 4.2 ka BP event that is still underrepresented in environmental studies from the LOR. Frequently discussed as one of the most severe drought episodes of the Holocene epoch in semiarid regions, the interval around 4200 a BP and the following period in the RZ19 record does not indicate drier environments near Lake Onega. This may indicate spatial differences in the distribution and seasonality of precipitation across Europe, as supported by modelling experiments.

Data availability

The data are available on request from the corresponding authors.

Funding

The work of AIK and FK is financially supported through doctoral stipends granted by the Freie Universität Berlin (FUB), University of Alberta and the Social Sciences and Humanities Research Council of Canada for the project "Individual life histories in long-term culture change: Holocene hunter-gatherers in Northern Eurasia" (SSHRC Partnership Grant No. 895-2018-1004). TL's work was supported by the UNNC seed funding (Grant No. RESI202209004) and Major Humanities and Social Sciences Research Projects in Zhejiang higher education institutions (Grant No. 2023QN032).

CRediT authorship contribution statement

Aleksandra I. Krikunova: Conceptualization, Data curation, Formal analysis, Investigation, Methodology, Validation, Visualization, Writing – original draft, Writing – review & editing. **Larisa A. Savelieva:** Conceptualization, Investigation, Methodology, Project administration, Resources, Supervision, Writing – review & editing. **Tengwen Long:** Investigation, Methodology, Software, Visualization, Writing – original draft. **Christian Leipe:** Validation, Writing – review & editing. **Franziska Kobe:** Investigation, Methodology. **Natalia A. Kostromina:** Data curation, Investigation. **Aleksandra V. Vasilyeva:** Investigation, Methodology, Writing – review & editing. **Pavel E. Tarasov:** Conceptualization, Funding acquisition, Project administration, Resources, Supervision, Validation, Writing – review & editing.

Declaration of competing interest

The authors declare that they have no known competing financial interests or personal relationships that could have appeared to influence the work reported in this paper.

Acknowledgements

PET dedicates his contribution to Alla N. Varushchenko, a constant supporter of young scientists, a passionate palaeogeographer and an active promoter of interdisciplinary geoarchaeological research in Northern Eurasia, who passed away in June 2023. The authors thank the handling editor and two anonymous reviewers for their helpful suggestions.

Appendix A. Supplementary data

Supplementary data to this article can be found online at https://doi.org/10.1016/j.quaint.2024.04.003.

References

Abraham, V., Hicks, S., Svobodová-Svitavská, H., Bozilova, E., Panajiotidis, S., Filipova-Marinova, M., Jensen, C.E., Tonkov, S., Pidek, I.A., Święta-Musznicka, J., Zimny, M., Kvavadze, E., Filbrandt-Czaja, A., Hättestrand, M., Karlıoğlu Kılıç, N., Kosenko, J., Nosova, M., Severova, E., Volkova, O., Hallsdóttir, M., Kalniņa, L., Noryśkiewicz, A. M., Noryśkiewicz, B., Pardoe, H., Christodoulou, A., Koff, T., Fontana, S.L., Alenius, T., Isaksson, E., Seppä, H., Veski, S., Pędziszewska, A., Weiser, M., Giesecke, T., 2021. Patterns in recent and Holocene pollen accumulation rates across Europe – the Pollen Monitoring Programme Database as a tool for vegetation reconstruction. Biogeosci. 18 (15), 4511–4534. https://doi.org/10.5194/bg-18-4511-2021.

Alenius, T., Marquer, L., Molinari, C., Heikkilä, M., Ojala, A., 2021. The environment they lived in: anthropogenic changes in local and regional vegetation composition in eastern Fennoscandia during the Neolithic. Veg. Hist. Archaeobotany 30, 489–506. https://doi.org/10.1007/s00334–020–00796–w.

Allen, J.R.M., Long, A.J., Ottley, C.J., Pearson, D.G., Huntley, B., 2007. Holocene climate variability in northernmost Europe. Quat. Sci. Rev. 26, 1432–1453. https://doi.org/10.1016/j.quascirev.2007.02.009.

Alley, R.B., Mayewski, P.A., Sowers, T., Stuiver, M., Taylor, K.C., Clark, P.U., 1997. Holocene climatic instability: a prominent, widespread event 8200 yr ago. Geology 25 (6), 483–486. https://doi.org/10.1130/0091-7613(1997)025<0483:HCIAPW>2.3.CO;2.

Alpat'ev, A.M., Arkhangel'skii, A.M., Podoplelov, N.Y., Stepanov, A.Y., 1976. Physical Geography of the USSR (The European Part). Vysshaya Shkola, Moscow (in Russian).

Berglund, B.E., Birks, H.J.B., Ralska-Jasiewiczowa, M., Wright, H.E. (Eds.), 1996. Palaeoecological Events during the Last 15,000 Years: Regional Syntheses of Palaeoecological Studies of Lakes and Mires in Europe. Wiley, Chichester.

Binney, H.A., Willis, K.J., Edwards, M.E., Bhagwat, S.A., Anderson, P.M., Andreev, A.A., Blaauw, M., Damblon, F., Haesaerts, P., Kienast, F., Kremenetski, K.V., Krivogonov, S.K., Lozhkin, A.V., MacDonald, G.M., Novenko, E.Y., Oksanen, P., Sapelko, N.V., Väliranta, M., Vazhenina, L., 2009. The distribution of late-Quaternary woody taxa in northern Eurasia: evidence from a new macrofossil database. Quat. Sci. Rev. 28, 2445–2464. https://doi.org/10.1016/j.quascirev.2009.04.016.

Binney, H., Edwards, M., Macias-Fauria, M., Lozhkin, A., Anderson, P., Kaplan, J.O., Andreev, A., Bezrukova, E., Blyakharchuk, T., Jankovska, V., Khazina, I., Krivonogov, S., Kremenetski, K., Nield, J., Novenko, E., Ryabogina, N., Solovieva, N., Willis, K., Zernitskaya, V., 2017. Vegetation of Eurasia from the last glacial maximum to present: key biogeographic patterns. Quat. Sci. Rev. 157, 80–97. https://doi.org/10.1016/j.quascirev.2016.11.022.

Blaauw, M., Christen, J.A., 2011. Flexible paleoclimate age-depth models using an autoregressive gamma process. Bayesian Analysis 6, 457–474. https://doi.org/10.1214/ba/1339616472.

Bobrov, A.Y., Kupriyanova, L.A., Litvintseva, M.V., Tarasevitch, V.F., 1983. Fern Spores and Monocotyledonous and Gymnosperm Pollen from the Flora of the European Part of the USSR. Nauka, Leningrad (in Russian).

Bronk Ramsey, C., 1995. Radiocarbon calibration and analysis of stratigraphy: the OxCal program. Radiocarbon 37 (2), 425–430. https://doi.org/10.1017/S0033822200030903.

Bronk Ramsey, C., Schulting, R., Goriunova, O.I., Bazaliiskii, V.I., Weber, A.W., 2014. Analyzing radiocarbon reservoir offsets through stable nitrogen isotopes and Bayesian modeling: a case study using paired human and faunal remains from the Cis–Baikal region, Siberia. Radiocarbon 56 (2), 789–799. https://doi.org/10.2458/56.17160.

Clear, J.L., Molinari, C., Bradshaw, R.H.W., 2014. Holocene fire in Fennoscandia and Denmark. Int. J. Wildland Fire 23 (6), 781–789. https://doi.org/10.1071/WF13188.

Crawford, R.M.M., Jeffree, C.E., Rees, W.G., 2003. Paludification and forest retreat in northern oceanic environments. Ann. Bot. 91, 213–226. https://doi.org/10.1093/aob/mcf185.

DeMenocal, P.B., 2001. Cultural responses to climate change during the late Holocene. Science 292 (5517), 667–673. https://doi.org/10.1126/science.1059287.

Demidov, I.N., 2005. Degradation of the last glaciation in Lake Onega basin. Geol. Miner. Resour. Karelia 8, 134–142 (in Russian).

Demidov, I.N., 2006. On a maximum stage in the evolution of periglacial Lake Onega, variations in its level and the glacioisostatic shore uplift in the Late Glacial Period. Geol. Miner. Resour. Karelia 9, 171–180 (in Russian).

Dixit, Y., Hodell, D.A., Petrie, C.A., 2014a. Abrupt weakening of the summer monsoon in northwest India ~ 4100 yr ago. Geology 42 (4), 339–342.

Dixit, Y., Hodell, D.A., Sinha, R., Petrie, C.A., 2014b. Abrupt weakening of the Indian summer monsoon at 8.2 kyr B.P. Earth Planet. Sci. Lett. 391, 16–23. https://doi.org/10.1016/j.epsl.2014.01.026.

Edwards, M.E., Anderson, P.M., Brubaker, L.B., Ager, T.A., Andreev, A.A., Bigelow, N.H., Cwynar, L.C., Eisner, W.R., Harrison, S.P., Hu, F.S., Jolly, D., Lozhkin, A.V., MacDonald, G.M., Mock, C.J., Ritchie, J.C., Sher, A.V., Spear, R.W., Williams, J.W., Yu, G., 2000. Pollen-based biomes for Beringia 18,000, 6000 and 0 14C yr BP. J. Biogeogr. 27 (3), 521–554. https://doi.org/10.1046/j.1365-2699.2000.00426.x.

Elina, G.A., Khomutova, V.I., 1987. Correlation of Holocene sequences of bottom sediments from Onega Lake and its old bays in terms of palynological data. In: Kabailiene, M. (Ed.), Methods for the Investigation of Lake Deposits: Palaeoecological and Palaeoclimatological Aspects. V. Kapsukas Univ., Vilnius, pp. 193–203.

Elina, G.A., Lukashov, A.D., Yurkovskaya, T.K., 2010. Late Glacial and Holocene Palaeovegetation and Palaeogeography of Eastern Fennoscandia. Finnish Environment Institute, Helsinki.

Erästö, P., Holmström, L., Korhola, A., Weckström, J., 2012. Finding a consensus on credible features among several paleoclimate reconstructions. Ann. Appl. Stat. 6 (4), 1377–1405. https://doi.org/10.1214/12-AOAS540.

Fægri, K., Iversen, J., 1989. Textbook of Pollen Analysis. Wiley, Chichester.

Filatov, N.N. (Ed.), 2010. Onezhskoye Ozero. Atlas. KarRC RAS, Petrozavodsk (in Russian).

Filimonova, L.V., Lavrova, N.B., 2015. Paleogeography of the Zaonezhye Peninsula in the late Pleistocene and Holocene. Trans. KarRC RAS 4, 30–47. https://doi.org/10.17076/bg22 (in Russian).

Filimonova, L.V., Lavrova, N.B., 2017. The study of Lake Onega and its drainage basin paleogeography using a set of methods. Proc. KarRC RAS 10, 86–100. https://doi.org/10.17076/lim703 (in Russian).

Filoc, M., Kupryjanowicz, M., Szeroczyńska, K., Suchora, M., Rzodkiewicz, M., 2017. Environmental changes related to the 8.2-ka event and other climate fluctuations during the middle Holocene: evidence from two dystrophic lakes in NE Poland. Holocene 27, 1550–1566. https://doi.org/10.1177/0959683617702233.

Gerasimov, D., Kriiska, A., 2018. Early-Middle Holocene archaeological periodization and environmental changes in the Eastern Gulf of Finland: interpretative correlation. Quat. Int. 465, 238–313. https://doi.org/10.1016/j.quaint.2016.12.011.

Ghilardi, B., O'Connell, M., 2013. Early Holocene vegetation and climate dynamics with particular reference to the 8.2 ka event: pollen and macrofossil evidence from a small lake in western Ireland. Veg. Hist. Archaeobotany 22, 99–114. https://doi.org/10.1007/s00334-012-0367-x.

Giesecke, T., Bennett, K.D., 2004. The Holocene spread of *Picea abies* (L.) Karst. in Fennoscandia and adjacent areas. J. Biogeogr. 31 (9), 1523–1548. https://doi.org/10.1111/j.1365-2699.2004.01095.x.

Grimm, E.C., 1987. CONISS: a FORTRAN 77 program for stratigraphically constrained cluster analysis by the method of incremental sum of squares. Comput. Geosci. 13 (1), 13–35. https://doi.org/10.1016/0098-3004(87)90022-7.

Grimm, E.C., 2011. Tilia 1.7.16 Software. Illinois State Museum. RCC, Springfield.

Harrison, S.P., Yu, G.E., Tarasov, P.E., 1996. Late Quaternary lake-level record from northern Eurasia. Quat. Res. 45 (2), 138–159. https://doi.org/10.1006/qres.1996.0016.

Head, M.J., 2019. Formal subdivision of the Quaternary System/Period: present status and future directions. Quat. Int. 500, 32–51. https://doi.org/10.1016/j.quaint.2019.05.018.

Henne, P.D., Elkin, C.M., Reineking, B., Bugmann, H., Tinner, W., 2011. Did soil development limit spruce (*Picea abies*) expansion in the Central Alps during the Holocene? Testing a palaeobotanical hypothesis with a dynamic landscape model. J. Biogeogr. 38 (5), 933–949. https://doi.org/10.1111/j.1365-2699.2010.02460.x.

Houston Durrant, T., de Rigo, D., Caudullo, G., 2016. *Alnus incana* in Europe: distribution, habitat, usage and threats. In: San-Miguel-Ayanz, J., de Rigo, D., Caudullo, G., Houston Durrant, T., Mauri, A. (Eds.), European Atlas of Forest Tree Species. Publ. Off. EU, Luxembourg, pp. 66-67.

Hughes, A.L.C., Gyllencreutz, R., Lohne, Ø.S., Mangerud, J., Svendsen, J.I., 2016. The last Eurasian ice sheets – a chronological database and time-slice reconstruction, DATED-1. Boreas 45, 1–45. https://doi.org/10.1111/bor.12142.

Kageyama, M., Peyron, O., Pinot, S., Tarasov, P., Guiot, J., Joussaume, S., Ramstein, G., participating groups, P.M.I.P., 2001. The Last Glacial Maximum climate over Europe and western Siberia: a PMIP comparison between models and data. Clim. Dyn. 17, 23–43. https://doi.org/10.1007/s003820000095.

Kaufman, D.S., Broadman, E., 2023. Revisiting the Holocene global temperature conundrum. Nature 614 (7948), 425–435. https://doi.org/10.1038/s41586-022-05536-w.

Knight, C.A., Battles, J.J., Bunting, M.J., Champagne, M., Wanket, J.A., Wahl, D.B., 2022. Methods for robust estimates of tree biomass from pollen accumulation rates: quantifying paleoecological reconstruction uncertainty. Front. Ecol. Evol. 10, 956143 https://doi.org/10.3389/fevo.2022.956143.

Köppen, W., 1923. Die Klimate der Erde: Grundriss der Klimakunde. De Gruyter, Berlin, Boston.

Kotlyakov, V.M., Velichko, A.A., Vasil'ev, S.A. (Eds.), 2017. Human Colonization of the Arctic: the Interaction between Early Migration and the Paleoenvironment. Academic Press, Amsterdam and New York.

Kottek, M., Grieser, J., Beck, C., Rudolf, B., Rubel, F., 2006. World Map of the Köppen-Geiger climate classification updated. Meteorol. Z. 15 (3), 259–263. https://doi.org/10.1127/0941-2948/2006/0130.

Kremenetski, C.V., Sulerzhitsky, L.D., Hantemirov, R., 1998. Holocene history of the northern range limits of some trees and shrubs in Russia. Arct. Antarct. Alp. Res. 30 (4), 317–333.

Krikunova, A.I., Kostromina, N.A., Savelieva, L.A., Tolstobrov, D.S., Petrov, A.Y., Long, T., Kobe, F., Leipe, C., Tarasov, P.E., 2022. Late- and postglacial vegetation and climate history of the central Kola Peninsula derived from a radiocarbon-dated pollen record of Lake Kamenistoe. Palaeogeogr. Palaeoclimatol. Palaeoecol. 603, 111191 https://doi.org/10.1016/j.palaeo.2022.111191.

Kupriyanova, L.A., Aleshina, L.A., 1972. Pollen and Spores of Plants of the Flora of the European Part of the USSR, vol. 1. Nauka, Leningrad (in Russian).

Kupriyanova, L.A., Aleshina, L.A., 1978. Pollen and Spores of Plants of the Flora of the European Part of the USSR, vol. 2. Nauka, Leningrad (in Russian).

Lavrova, N.B., 2005. Development of the vegetation in the Lake Onega basin during degradation of the late glaciation. Geol. Miner. Resour. Karelia 8, 143–148 (in Russian).

Lenz, M., Savelieva, L., Frolova, L., Cherezova, A., Moros, M., Baumer, M.M., Gromig, R., Kostromina, N., Nigmatullin, N., Kolka, V., Wagner, B., Fedorov, G., Melles, M., 2021. Lateglacial and Holocene environmental history of the central Kola region, northwestern Russia revealed by a sediment succession from Lake Imandra. Boreas 50, 76–100. https://doi.org/10.1111/bor.12465.

Li, H., Renssen, H., Roche, D.M., Miller, P.A., 2019. Modelling the vegetation response to the 8.2 ka BP cooling event in Europe and Northern Africa. J. Quat. Sci. 34 (8), 650–661. https://doi.org/10.1002/jqs.3157.
Lindholm, T., Jakovlev, J., Kravchenko, A., 2015. Biogeography, Landscapes, Ecosystems and Species of Zaonezhye Peninsula, in Lake Onega, Russian Karelia. SYKE, Helsinki.
Lunkka, J.P., Kaparulina, E., Putkinen, N., Saarnisto, M., 2018. Late Pleistocene palaeoenvironments and the last deglaciation on the Kola Peninsula, Russia. Arktos 4, 1–18. https://doi.org/10.1007/s41063-018-0053-z.
Magny, M., Combourieu–Nebout, N., De Beaulieu, J.L., Bout-Roumazeilles, V., Colombaroli, D., Desprat, S., Francke, A., Joannin, S., Ortu, E., Peyron, O., Revel, M., Sadori, L., Siani, G., Sicre, M.A., Samartin, S., Simonneau, A., Tinner, W., Vannière, B., Wagner, B., Zanchetta, G., Anselmetti, F., Brugiapaglia, E., Chapron, E., Debret, M., Desmet, M., Didier, J., Essallami, L., Galop, D., Gilli, A., Haas, J.N., Kallel, N., Millet, L., Stock, A., Turon, J.L., Wirth, S., 2013. North-south palaeohydrological contrasts in the central Mediterranean during the Holocene: tentative synthesis and working hypotheses. Clim. Past 9 (5), 2043–2071. https://doi.org/10.5194/cp-9-2043-2013.
Manninen, M.A., Tallavaara, M., Seppä, H., 2018. Human responses to early Holocene climate variability in eastern Fennoscandia. Quat. Int. 465 (Part B), 287–297. https://doi.org/10.1016/j.quaint.2017.08.043.
Matero, S.O., Gregoire, L.J., Ivanovic, R.F., Tindall, J.C., Haywood, A.M., 2017. The 8.2 ka cooling event caused by Laurentide ice saddle collapse. Earth Planet Sci. Lett. 473, 205–214. https://doi.org/10.1016/j.epsl.2017.06.011.
Mauri, A., Davis, B.A.S., Collins, P.M., Kaplan, J.O., 2015. The climate of Europe during the Holocene: a gridded pollen-based reconstruction and its multi-proxy evaluation. Quat. Sci. Rev. 112, 109–127. https://doi.org/10.1016/j.quascirev.2015.01.013.
Meyer-Jacob, C., Bindler, R., Bigler, C., Leng, M.J., Lowick, S.E., Vogel, H., 2017. Regional Holocene climate and landscape changes recorded in the large subarctic lake Torneträsk, N Fennoscandia. Palaeogeogr. Palaeoclimatol. Palaeoecol. 487, 1–14. https://doi.org/10.1016/j.palaeo.2017.08.001.
Mishra, S., Tripathi, A., Tripathi, D.K., Chauhan, D.K., 2016. Role of sedges (Cyperaceae) in wetlands, environmental cleaning and as food material: possibilities and future perspectives. In: Azooz, M.M., Ahmad, P. (Eds.), Plant-environment Interaction: Responses and Approaches to Mitigate Stress. Wiley, Chichester, pp. 327–338. https://doi.org/10.1002/9781119081005.ch18.
Mokhova, L., Tarasov, P., Bazarova, V., Klimin, M., 2009. Quantitative biome reconstruction using modern and late Quaternary pollen data from the southern part of the Russian Far East. Quat. Sci. Rev. 28 (25–26), 2913–2926. https://doi.org/10.1016/j.quascirev.2009.07.018.
Moore, P.D., Webb, J.A., Collinson, M.E., 1991. Pollen Analysis. Blackwell, Oxford.
Nakagawa, T., Tarasov, P., Staff, R., Bronk Ramsey, C., Marshall, M., Schlolaut, G., Bryant, C., Brauer, A., Lamb, H., Haraguchi, T., Gotanda, K., Kitaba, I., Kitagawa, H., van der Plicht, J., Yonenobu, H., Omori, T., Yokoyama, Y., Tada, R., Yasuda, Y., Suigetsu 2006 Project Members, 2021. The spatio-temporal structure of the Lateglacial to early Holocene transition reconstructed from the pollen record of Lake Suigetsu and its precise correlation with other key global archives: implications for palaeoclimatology and archaeology. Global Planet. Change 202, 103493. https://doi.org/10.1016/j.gloplacha.2021.103493.
Nazarova, L., Syrykh, L., Mayfield, R.J., Frolova, L., Ibragimova, A., Grekov, I., Subetto, D., 2020. Palaeoecological and palaeoclimatic conditions on the Karelian Isthmus (northwestern Russia) during the Holocene. Quat. Res. 95, 65–83. https://doi.org/10.1017/qua.2019.88.
Parfenova, E.I., Kuzmina, N.A., Kuzmin, S.R., Tchebakova, N.M., 2021. Climate warming impacts on distributions of Scots pine (*Pinus sylvestris* L.) seed zones and seed mass across Russia in the 21st century. Forests 12, 1097. https://doi.org/10.3390/f12081097.
Parker, S.E., Harrison, S.P., 2022. The timing, duration and magnitude of the 8.2 ka event in global speleothem records. Sci. Rep. 12 (1), 10542 https://doi.org/10.1038/s41598-022-14684-y.
Paus, A., Haflidason, H., Routh, J., Naafs, B.D.A., Thoen, M.W., 2019. Environmental responses to the 9.7 and 8.2 cold events at two ecotonal sites in the Dovre mountains, mid-Norway. Quat. Sci. Rev. 205, 45–61. https://doi.org/10.1016/j.quascirev.2018.12.009.
Plikk, A., Engels, S., Luoto, T.P., Nazarova, L., Salonen, J.S., Helmens, K.F., 2019. Chironomid–based temperature reconstruction for the Eemian Interglacial (MIS 5e) at Sokli, northeast Finland. J. Paleolimnol. 61 (3), 355–371. https://doi.org/10.1007/s10933-018-00064-y.
Prentice, I.C., Cramer, W., Harrison, S.P., Leemans, R., Monserud, R.A., Solomon, A.M., 1992. A global biome model based on plant physiology and dominance, soil properties and climate. J. Biogeogr. 19, 117–134. https://doi.org/10.2307/2845499.
Prentice, I.C., Guiot, J., Huntley, B., Jolly, D., Cheddadi, R., 1996. Reconstructing biomes from palaeoecological data: a general method and its application to European pollen data at 0 and 6 ka. Clim. Dyn. 12, 185–194. https://doi.org/10.1007/BF00211617.
Prentice, I.C., Webb III, T., 1998. Biome 6000: reconstructing global mid-Holocene vegetation patterns from palaeoecological records. J. Biogeogr. 25, 997–1005. https://www.jstor.org/stable/2846196.
R Core Team, 2016. R: A Language and Environment for Statistical Computing. R Foundation for Statistical Computing, Vienna, Austria.
Reimer, P.J., Austin, W.E.N., Bard, E., Bayliss, A., Blackwell, P.G., Bronk Ramsey, C., Butzin, M., Cheng, H., Edwards, R.L., Friedrich, M., Grootes, P.M., Guilderson, T.P., Hajdas, I., Heaton, T.J., Hogg, A.G., Hughen, K.A., Kromer, B., Manning, S.W., Muscheler, R., Palmer, J.G., Pearson, C., van der Plicht, J., Reimer, R.W., Richards, D.A., Scott, E.M., Southon, J.R., Turney, C.S.M., Wacker, L., Adolphi, F., Büntgen, U., Capano, M., Fahrni, S.M., Fogtmann–Schulz, A., Friedrich, R., Köhler, P., Kudsk, S., Miyake, F., Olsen, J., Reinig, F., Sakamoto, M., Sookdeo, A., Talamo, S., 2020. The IntCal20 Northern Hemisphere radiocarbon age calibration curve (0-55 cal kBP). Radiocarbon 62, 725–757. https://doi.org/10.1017/RDC.2020.41.
Roberts, N., Fyfe, R.M., Woodbridge, J., Gaillard, M.J., Davis, B.A., Kaplan, J.O., Marquer, L., Mazier, F., Nielsen, A.B., Sugita, S., Trondman, A.-K., Leydet, M., 2018. Europe's lost forests: a pollen-based synthesis for the last 11,000 years. Sci. Rep. 8 (1), 716. https://doi.org/10.1038/s41598-017-18646-7.
Rohling, E.J., Pälike, H., 2005. Centennial-scale climate cooling with a sudden cold event around 8200 years ago. Nature 434 (7036), 975–979. https://doi.org/10.1038/nature03421.
Roland, T.P., Caseldine, C.J., Charman, D.J., Turney, C.S., Amesbury, M.J., 2014. Was there a '4.2 ka event' in Great Britain and Ireland? Evidence from the peatland record. Quat. Sci. Rev. 83, 11–27. https://doi.org/10.1016/j.quascirev.2013.10.024.
Saarnisto, M., Grönlund, T., Ekman, I., 1995. Lateglacial of Lake Onega – contribution to the history of the eastern baltic basin. Quat. Int. 27, 111–120. https://doi.org/10.1016/1040-6182(95)00068-T.
Saarnisto, M., Saarinen, T., 2001. Deglaciation chronology of the scandinavian ice sheet from the Lake Onega basin to the salpausselkä end moraines. Global Planet. Change 31, 387–405. https://doi.org/10.1016/S0921-8181(01)00131-X.
Savelieva, L.A., 2010. A cartographical model of the Holocene expansion of spruce on the north-west Russian plain. In: Yurkovskaya, T.K. (Ed.), Research Problems and Goals in Modern Mire Science in Russia. BIN RAS, Saint Petersburg (in Russian).
Savelieva, L.A., Raschke, E.A., Titova, D.V., 2013. Photographic Atlas of Plants and Pollen of the Lena River Delta. St. Petersburg State University, St. Petersburg (in Russian).
Schulting, R.J., Mannermaa, K., Tarasov, P.E., Higham, T., Ramsey, C.B., Khartanovich, V., Moiseyev, V., Gerasimov, D., O'Shea, J., Weber, A., 2022. Radiocarbon dating from Yuzhniy Oleniy Ostrov cemetery reveals complex human responses to socio-ecological stress during the 8.2 ka cooling event. Nat. Ecol. Evol. 6 (2), 155–162. https://doi.org/10.1038/s41559-021-01628-4.
Seppä, H., Birks, H.J.B., Giesecke, T., Hammarlund, D., Alenius, T., Antonsson, K., Bjune, A.E., Heikkilä, M., MacDonald, G.M., Ojala, A.E.K., Telford, R.J., Veski, S., 2007. Spatial structure of the 8200 cal. yr BP event in northern Europe. Clim. Past 3 (2), 225–236. https://doi.org/10.5194/cp-3-225-2007.
Seppä, H., Bjune, A.E., Telford, R.J., Birks, H.J.B., Veski, S., 2009. Last nine-thousand years of temperature variability in Northern Europe. Clim. Past 5 (3), 523–535. https://doi.org/10.5194/cp-5-523-2009.
Sharov, A.N., Berezina, N.A., Nazarova, L.E., Poliakova, T.N., Chekryzheva, T.A., 2014. Links between biota and climate-related variables in the Baltic region using Lake Onega as an example. Oceanologia 56 (2), 291–306. https://doi.org/10.5697/oc.56-2.291.
Shevelin, P.F., Elina, G.A., Khomutova, V.I., Arslanov, KhA., 1988. Reflection of fluctuations of the level regime of Lake Onega in the vegetation and stratigraphy of Razlomnoe peatbog in the Holocene. In: Lopatin, V.D. (Ed.), Bog Ecosystems of the European North. Karelian Branch AS USSR. Petrozavodsk, pp. 39–59 (in Russian).
Sokolov, S.Y., Svyzeva, O.A., Kubli, V.A., Kamelina, R.V., Yakovleva, G.P., Grubova, V.P., 1986. Geographical Range of Trees and Shrubs of the USSR, vol. 3. Nauka, Leningrad (in Russian).
Stockmarr, J.A., 1971. Tablets with spores used in absolute pollen analysis. Pollen Spores 13, 615–621.
Stroeven, A.P., Hättestrand, C., Kleman, J., Heyman, J., Fabel, D., Fredin, O., Goodfellow, B.W., Harbor, J.M., Jansen, J.D., Olsen, L., Caffee, M., Fink, D., Lundqvist, J., Rosqvist, G., Strömberg, B., Jansson, K., 2016. Deglaciation of Fennoscandia. Quat. Sci. Rev. 147, 91–121. https://doi.org/10.1016/j.quascirev.2015.09.016.
Sun, A., Luo, Y., Wu, H., Chen, X., Li, Q., Yu, Y., Sun, X., Guo, Z., 2020. An updated biomization scheme and vegetation reconstruction based on a synthesis of modern and mid-Holocene pollen data in China. Global Planet. Change 192, 103178. https://doi.org/10.1016/j.gloplacha.2020.103178.
Svendsen, J.I., Alexanderson, H., Astakhov, V.I., 2004. Late Quaternary ice sheet history of northern Eurasia. Quat. Sci. Rev. 23, 1229–1271. https://doi.org/10.1016/j.quascirev.2003.12.008.
Svensson, A., Andersen, K.K., Bigler, M., Clausen, H.B., Dahl-Jensen, D., Davies, S.M., Johnsen, S.J., Muscheler, R., Parrenin, F., Rasmussen, S.O., Röthlisberger, R., Seierstad, I., Steffensen, J.P., Vinther, B.M., 2008. A 60,000 year Greenland stratigraphic ice core chronology. Clim. Past 4 (1), 47–57. https://doi.org/10.5194/cp-4-47-2008.
Tallavaara, M., Pesonen, P., Oinonen, M., 2010. Prehistoric population history in eastern Fennoscandia. J. Archaeol. Sci. 37, 251–260. https://doi.org/10.1016/j.jas.2009.09.035.
Tan, L., Li, Y., Wang, X., Cai, Y., Lin, F., Cheng, H., Ma, L., Sinha, A., Edwards, R.L., 2020. Holocene monsoon change and abrupt events on the western Chinese Loess Plateau as revealed by accurately dated stalagmites. Geophys. Res. Lett. 47 (21), e2020GL090273 https://doi.org/10.1029/2020GL090273.
Tarasov, A.Yu., Nordqvist, K., Mökkönen, T., Khoroshun, T., 2017. Radiocarbon chronology of the Neolithic-Eneolithic period in the Karelian republic (Russia). Doc. Praehist. 44, 98–121. https://doi.org/10.4312/dp.44.7.
Tarasov, P.E., Webb III, T., Andreev, A.A., Afanas'eva, N.B., Berezina, N.A., Bezusko, L.G., Blyakharchuk, T.A., Bolikhovskaya, N.S., Cheddadi, R., Chernavskaya, M.M., Chernova, G.M., Dorofeyuk, N.I., Dirksen, V.G., Elina, G.A., Filimonova, L.V., Glebov, F.Z., Guiot, J., Gunova, V.S., Harrison, S.P., Jolly, D., Khomutova, V.I., Kvavadze, E.V., Osipova, I.M., Panova, N.K., Prentice, I.C., Saarse, L., Sevastyanov, D.V., Volkova, V.S., Zernitskaya, V.P., 1998. Present-day and mid-Holocene biomes reconstructed from pollen and plant macrofossil data from the former Soviet Union and Mongolia. J. Biogeogr. 25, 1029–1053. https://doi.org/10.1046/j.1365-2699.1998.00236.x.

Tarasov, P.E., Andreev, A.A., Anderson, P.M., Lozhkin, A.V., Leipe, C., Haltia, E., Nowaczyk, N.R., Wennrich, V., Brigham–Grette, J., Melles, M., 2013. A pollen-based biome reconstruction over the last 3.562 million years in the Far East Russian Arctic – new insights into climate-vegetation relationships at the regional scale. Clim. Past 9, 2759–2775. https://doi.org/10.5194/cp-9-2759-2013.

Tarasov, P.E., Savelieva, L.A., Kobe, F., Korotkevich, B.S., Long, T., Kostromina, N.A., Leipe, C., 2022. Lateglacial and Holocene changes in vegetation and human subsistence around Lake Zhizhitskoye, East European midlatitudes, derived from radiocarbon-dated pollen and archaeological records. Quat. Int. 623, 184–197. https://doi.org/10.1016/j.quaint.2021.06.027.

Väliranta, M., Kaakinen, A., Kuhry, P., Kultti, S., Salonen, J.S., Seppä, H., 2011. Scattered late-glacial and early Holocene tree populations as dispersal nuclei for forest development in north-eastern European Russia. J. Biogeogr. 38 (5), 922–932. https://doi.org/10.1111/j.1365-2699.2010.02448.x.

van Geel, B., 2001. Non-pollen palynomorphs. In: Smol, J.P., Birks, H.J.B., Last, W.M. (Eds.), Tracking Environmental Change Using Lake Sediments, Developments in Paleoenvironmental Research, vol. 3. Springer, Dordrecht. https://doi.org/10.1007/0-306-47668-1_6.

Velichko, A.A., Faustova, M.A., Pisareva, V.V., Karpukhina, N.V., 2017. History of the Scandinavian ice sheet and surrounding landscapes during Valday ice age and the Holocene. Ice Snow 57 (3), 391–416 (in Russian).

Veski, S., Seppä, H., Ojala, A.E., 2004. Cold event at 8200 yr BP recorded in annually laminated lake sediments in eastern Europe. Geology 32 (8), 681–684. https://doi.org/10.1130/G20683.1.

Vinther, B.M., Buchardt, S.L., Clausen, H.B., Dahl-Jensen, D., Johnsen, S.J., Fisher, D.A., Koerner, R.M., Raynaud, D., Lipenkov, V., Andersen, K.K., Blunier, T., 2009. Holocene thinning of the Greenland ice sheet. Nature 461 (7262), 385–388. https://doi.org/10.1038/nature08355.

Vuorela, I., Saarnisto, M., Lempiäinen, T., Taavitsainen, J.P., 2001. Stone age to recent land-use history at Pegrema, northern Lake Onega, Russian Karelia. Veg. Hist. Archaeobotany 10, 121–138.

Walker, M.J., Berkelhammer, M., Björck, S., Cwynar, L.C., Fisher, D.A., Long, A.J., Lowe, J.J., Newnham, R.M., Rasmussen, S.O., Weiss, H., 2012. Formal subdivision of the Holocene series/epoch: a discussion paper by a working group of INTIMATE (integration of ice-core, marine and terrestrial records) and the subcommission on quaternary stratigraphy (international commission on stratigraphy). J. Quat. Sci. 27 (7), 649–659. https://doi.org/10.1002/jqs.2565.

Walker, M., Head, M.J., Berkelhammer, M., Björck, S., Cheng, H., Cwynar, L., Fisher, D., Gkinis, V., Long, A., Lowe, J., Newnham, R., Rasmussen, S.O., Weiss, H., 2018. Formal ratification of the subdivision of the Holocene series/epoch (quaternary system/period): two new global boundary stratotype sections and points (GSSPs) and three new stages/subseries. Episodes J. Int. Geosci. 41 (4), 213–223. https://doi.org/10.18814/epiiugs/2018/018016.

Wang, Y., Goring, S.J., McGuire, J.L., 2019. Bayesian ages for pollen records since the last glaciation in North America. Sci. Data 6, 176. https://doi.org/10.1038/s41597-019-0182-7.

Wanner, H., Beer, J., Bütikofer, J., Crowley, T.J., Cubasch, U., Flückiger, J., Goosse, H., Grosjean, M., Joos, F., Kaplan, J.O., Küttel, M., Müller, S.A., Prentice, I.C., Solomina, O., Stocker, T.F., Tarasov, P., Wagner, M., Widmann, M., 2008. Mid- to late Holocene climate change: an overview. Quat. Sci. Rev. 27 (19–20), 1791–1828. https://doi.org/10.1016/j.quascirev.2008.06.013.

Werner, K., Tarasov, P.E., Andreev, A.A., Müller, S., Kienast, F., Zech, M., Zech, W., Diekmann, B., 2010. A 12.5-ka history of vegetation dynamics and mire development with evidence of the Younger Dryas larch presence in the Verkhoyansk Mountains, East Siberia, Russia. Boreas 39, 56–68. https://doi.org/10.1111/j.1502-3885.2009.00116.x.

Wiersma, A.P., Renssen, H., 2006. Model-data comparison for the 8.2 ka BP event: confirmation of a forcing mechanism by catastrophic drainage of Laurentide Lakes. Quat. Sci. Rev. 25 (1–2), 63–88. https://doi.org/10.1016/j.quascirev.2005.07.009.

Wohlfarth, B., Filimonova, L., Bennike, O., Björkman, L., Lavrova, N., Demidov, I., Possnert, G., 2002. Late-glacial and early Holocene environmental and climatic change at lake Tambichozero, southeastern Russian Karelia. Quat. Res. 58, 261–272. https://doi.org/10.1006/qres.2002.2386.

Wohlfarth, B., Schwark, L., Bennike, O., Filimonova, L., Tarasov, P., Björkmanj, L., Brunnberg, L., Demidov, I., Possnert, G., 2004. Unstable early-Holocene climatic and environmental conditions in northwestern Russia derived from a multidisciplinary study of a lake-sediment sequence from Pichozero, southeastern Russian Karelia. Holocene 14, 732–746. https://doi.org/10.1191/0959683604hl751rp.

Wohlfarth, B., Lacourse, T., Bennike, O., Subetto, D., Tarasov, P., Demidov, I., Filimonova, L., Sapelko, T., 2007. Climatic and environmental changes in north-western Russia between 15,000 and 8000 cal yr BP: a review. Quat. Sci. Rev. 26 (13–14), 1871–1883. https://doi.org/10.1016/j.quascirev.2007.04.005.

Yurkovskaya, T.K., 2011. Map of the vegetation. In: Shoba, S.A. (Ed.), National Atlas of Soils of the Russian Federation. Astrel, Moscow, pp. 46–47 (in Russian).